UCRL 3586
c. 2

UNIVERSITY OF CALIFORNIA

Radiation Laboratory

TWO-WEEK LOAN COPY

This is a Library Circulating Copy which may be borrowed for two weeks. For a personal retention copy, call Tech. Info. Division, Ext. 5545

BERKELEY, CALIFORNIA

DISCLAIMER

This document was prepared as an account of work sponsored by the United States Government. While this document is believed to contain correct information, neither the United States Government nor any agency thereof, nor the Regents of the University of California, nor any of their employees, makes any warranty, express or implied, or assumes any legal responsibility for the accuracy, completeness, or usefulness of any information, apparatus, product, or process disclosed, or represents that its use would not infringe privately owned rights. Reference herein to any specific commercial product, process, or service by its trade name, trademark, manufacturer, or otherwise, does not necessarily constitute or imply its endorsement, recommendation, or favoring by the United States Government or any agency thereof, or the Regents of the University of California. The views and opinions of authors expressed herein do not necessarily state or reflect those of the United States Government or any agency thereof or the Regents of the University of California.

UCRL-3586

UNIVERSITY OF CALIFORNIA

Radiation Laboratory
Berkeley, California

Contract No. W-7405-eng-48

CORRELATION OF LIMITING CURRENTS AT HORIZONTAL ELECTRODES UNDER FREE CONVECTION CONDITIONS

Eugene Joseph Fenech
(Master's Thesis)

November 1956

Printed for the U. S. Atomic Energy Commission

CORRELATION OF LIMITING CURRENTS AT HORIZONTAL ELECTRODES UNDER FREE CONVECTION CONDITIONS

Contents

Abstract 3
Introduction 4
Review of Heat Transfer from Horizontal Plates 5
The Present Problem 10
Experimental Apparatus and Proceedure 11
Discussion of Data 30
Correlation of Data 38
Discussion of Correlation 46
Conclusion 51
Acknowledgments 51
Appendix 1,
Calculation of Dimensionless Numbers 52
Appendix 2,
Equations for Prediction of Physical Properties 54
Appendix 3,
Purity of Chemicals 56
Nomenclature 57
List of Illustrations 59
Bibliography 61

CORRELATION OF LIMITING CURRENTS AT HORIZONTAL ELECTRODES UNDER FREE CONVECTION CONDITIONS

Eugene Joseph Fenech

Radiation Laboratory and Department of Chemical Engineering
University of California, Berkeley, California

ABSTRACT

Limiting currents were measured for flat, horizontal cathodes, facing upward in an unstirred cell. Electrolyte composition ranged from 0.01 to 0.7 M $CuSO_4$, in approximately 1.5 M H_2SO_4. Cathode sizes varied from 0.1 to 30 by 10 cm., and the free height above the electrode from 1 to 16 cm. Limiting currents were from 0.8 to 129 ma/cm^2. The data is best represented by the general correlation

$$Nu'' = 0.129 \ (Sc^{1.1} \ Gr)^{1/3},$$

where Nu", Sc, and Gr are the corrected mass transfer Nusselt number, Schmidt number, and Grashof number respectively. The experimental range included $10^8 < (Sc^{1.1} \ Gr) < 10^{13}$.

The results indicate that the analogy between mass and heat transfer can be extended to this model.

CORRELATION OF LIMITING CURRENTS AT HORIZONTAL ELECTRODES UNDER FREE CONVECTION CONDITIONS

Eugene Joseph Fenech

Radiation Laboratory and Department of Chemical Engineering
University of California, Berkeley, California

I. INTRODUCTION

In spite of the fact that free convection from horizontal surfaces is an important mode of mass transfer, there have been no papers, either theoretical or experimental, published on it. The difficulty of defining the motion and boundary conditions have rendered the mathematical treatment of this model virtually impossible. This work represents an initial effort, directed toward understanding the mechanism of mass transfer at horizontal surfaces.

In recent years, several important advances have been made in the quantitative interpretation of mass transfer phenomena in electrolytic processes. These have included studies of concentric, cylindrical rotating electrodes,[1] and of laminar and turbulent flow in channels, i.e., flow between parallel plate electrodes.[2] At both Eidg. Techn. Hochschule, in Zürich, and the University of California at Berkeley, research has been done on free convection at vertical electrodes. In Zürich, investigation of this model has been effected by means of interferometric studies of the boundary layer, and by observation on the electrodeposition of metallic powders.[3*] At Berkeley, the investigation centered about the determination of limiting current densities. By this method Wilke, Eisenberg, and Tobias[4] obtained the correlation

$$Nu' = 0.673 \ (Sc\ Gr)^{1/4} \qquad (1)$$

for electrodeposition at vertical electrodes in free convection. This equation was found to be valid over the range of Sc · Gr from 10^6 to 10^{12}. The quantities in the equations are defined by:

---

*Reference is to the summary paper.

$$Nu' = k_L X_f x / D \qquad (2)^*$$

$$Sc = \nu / D \qquad (3)$$

and

$$Gr = g (\rho_o - \rho_i) \rho^2 x^3 / \rho_i \mu^2 \qquad (4)$$

where x is the height of the electrode, and k_L is defined by the equation

$$k_L = I_L (1 - t_{Cu^{++}}) / n F C_o \qquad (5)$$

This correlation agrees very well with that derived from the analogous heat transfer case.[5] The only known observation on free convection mass transfer at horizontal electrodes were experiments performed by Wagner.**

Review of Heat Transfer from Horizontal Plates

The first experimental study on heat transfer from horizontal plates was carried out in 1900 by Henri Bénard,[6] when he studied the formation of certain patterns on the surface of liquids which were heated from below. His observations led him to believe that free convection produced definite cellular motions. The cells which he observed were hexagonal in shape with liquid rising in the center and decending at the edges. Figure 1, taken from Bénard's original paper, shows an elevation and a plan view of the cells. The occurance of such cells has also been noted in patterns on the surface of the sea and in cloud formations in the sky.[7]

Lord Rayleigh[8] was the first to attempt the analysis of heat transfer by free convection in Bénard cells from a mathematical point of view. The object of his study was to determine a minimum stability limit for the establishment and maintenance of the cellular convection

---

* For a detailed list of symbols, refer to nomenclature.

** These experiments were described in a private communication. Quantitative comparison is impossible, because of the qualitative nature of the data taken. However, the experimental results agree very well with those presented herein.

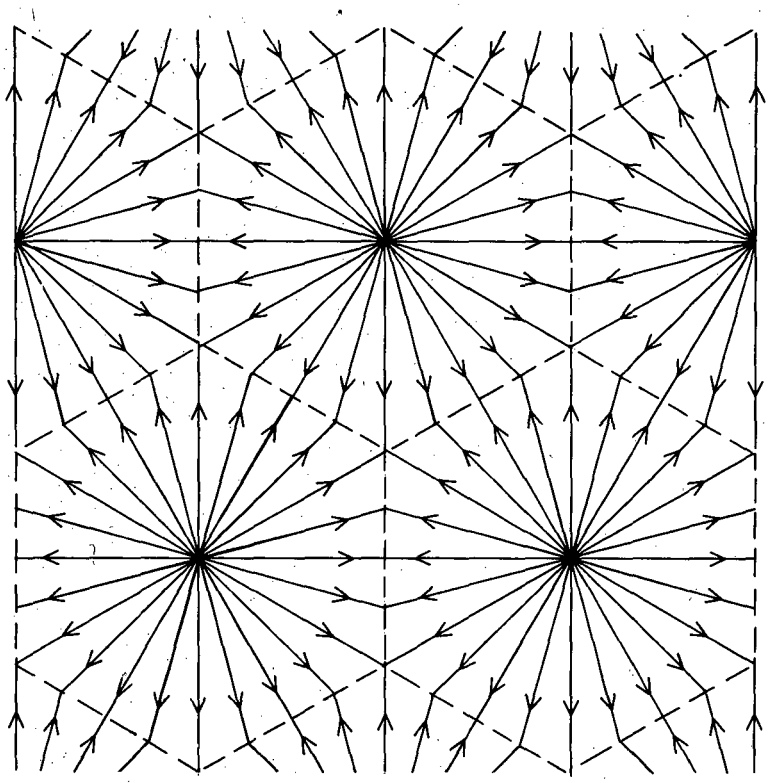

MU-12215

Fig. 1a. Plan view of schematic diagram of Bénard cells.

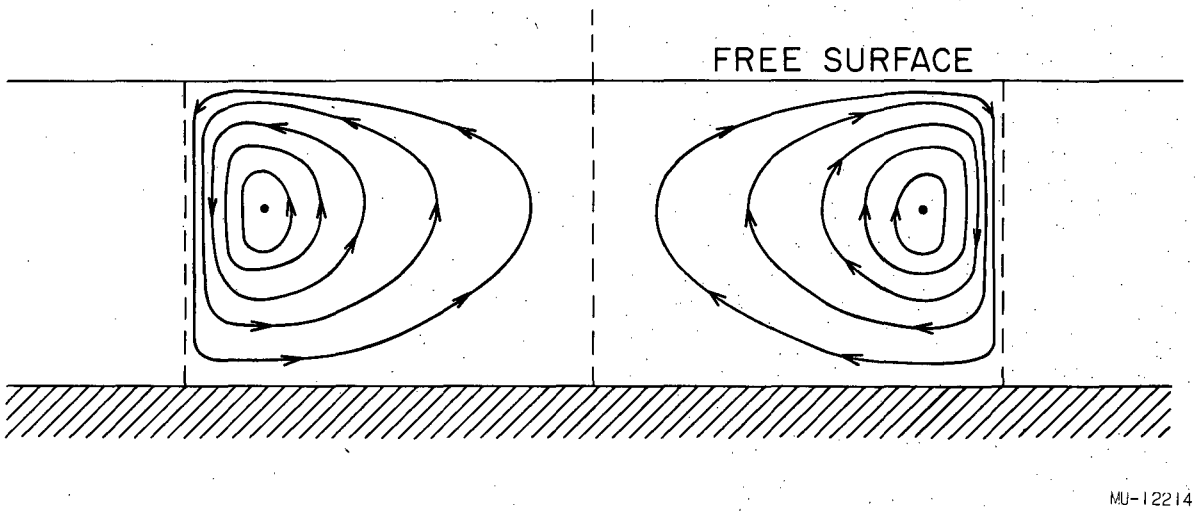

Fig. 1b. Elevation of schematic diagram of Bénard cells. The arrows give the direction of flow.

currents. The result of this mathematical analysis showed that if both the upper and lower boundries of the system were free, i.e., not rigid, convective cellular motion would be stable if the Rayleigh number exceeded 657.5, where

$$Ra = -\beta g \alpha x^4 / \kappa \nu \qquad (6)*$$

Further mathematical treatment in 1928 by Jeffreys[9] established the stability criterion, Rayleigh number equal 1707.8, for the case of both upper and lower boundaries being rigid. This type of mathematical proceedure was completed in 1940, when Pellew and Southwell[10] calculated the stability criterion, Rayleigh number equal 1100.7, for the case of one free and one rigid boundary.

In 1935, Schmidt and Milverton[11] experimentally verified the mathematical treatment of the rigid boundary model. Basically, their experiment consisted of transferring heat from a horizontal plate, which was electrically heated, through a liquid to a cooled plate directly above. Figure 2 shows one of the original diagrams. In it, the square of the heating current is plotted as a function of the temperature difference between the two plates. If the liquid properties are assumed to be independent of temperature, then for a given distance between plates current squared is proportional to the Nusselt number, and the temperature difference is proportional to the Rayleigh number. The break in the curve at Rayleigh number equal 1700, shows a change in mechanism of heat transfer. By visual methods it was observed that below 1700 there was no motion in the liquid, i.e., heat transfer occured by conduction only, and above 1700 the liquid motion was in the form of Bénard cells.

In 1938, this work was extended by Schmidt and Saunders[12] to much higher Rayleigh numbers. At Rayleigh numbers of approximately 45,000 another break in the curve (also shown on figure 2) was observed.** Visual observation showed that cellular flow broke up at this point and was replaced by a random turbulent boiling-like motion. Schmidt and

---

* It can be shown that the Rayleigh number is the product of the Prandtl and the Grashof numbers.

** On this second curve the break at Ra = 1700 is not shown.

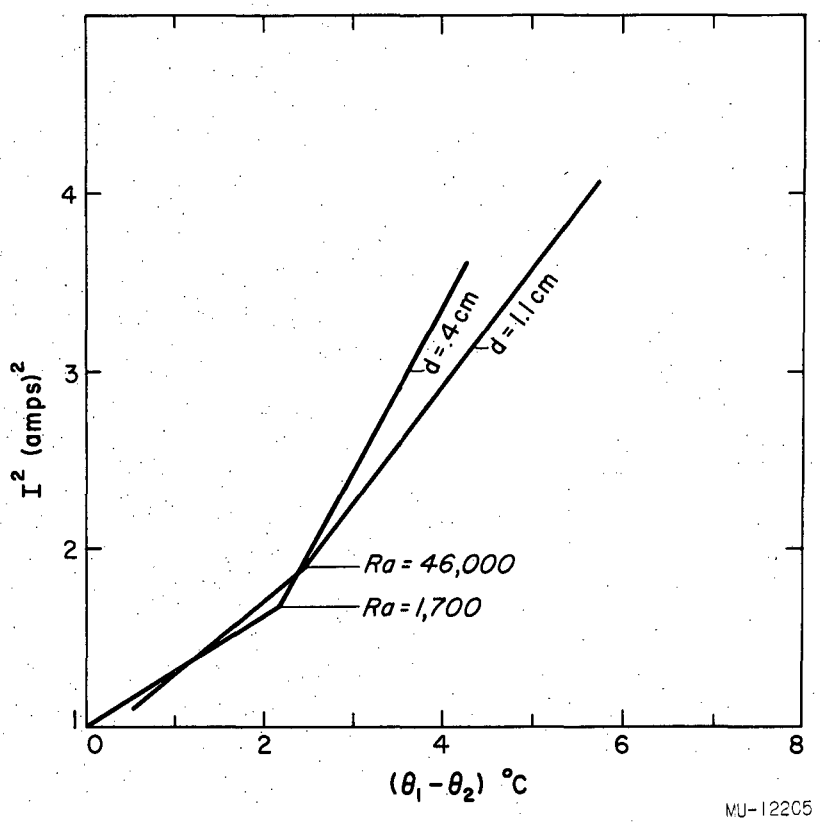

Fig. 2. Heating current squared as a function of temperature difference between plates in heat transfer for two different plate separations.

Saunders also noted that with water the shift from cellular flow to turbulent motion occurs very suddenly at 45,000, while with air the shift takes place in a transition zone beginning at Rayleigh numbers as low as 5,000.

W. V. R. Malkus,[13] in 1954, published a still further extension to this work. He studied systems up to Rayleigh numbers of 1.6×10^6, and in this range claims to have observed seven distinct breaks. However, after examining the graphs which he presents, it seems extremely fortuitous to be able to draw straight lines through sections of the data. It seems more probable that the data should be represented by a curved line, indicating a gradual change in the "degree" of turbulence rather than distinct changes in mechanism.

In 1956, Schmidt[14] reported on a number of heat transfer experiments conducted under free convection conditions. He included experiments on spheres, horizontal cylinders, and horizontal flat plates, using water, methanol, and ethylene glycol. As a result of this work, he suggests that a satisfactory correlation of heat transfer data in the turbulent region is possible in the form

$$Nu = a \left(Pr^{c} \cdot Gr \right)^{1/3} \tag{7}$$

where a and c are constants.

The latest addition to this field was made by Levy,[15] who presents a mathematical solution for the general heat transfer case. For a horizontal heated plate in the turbulent range, he suggests the following equation,

$$Nu = \frac{0.0727\ Gr^{4/11}\ Pr^{9/11}\ \left(x/D \right)^{1/11}}{\left(1 + 0.442\ Pr^{2/3} \right)^{4/11}} \tag{8}$$

However, this does not fit the case under investigation at present, because this model is a plate suspended in air with all surfaces actively contributing to the transfer.

The Present Problem

In the present work, limiting current densities were measured as functions of concentration of copper sulfate, viscosity (varied by adding glycerol to the solution), free height above the electrode, size of electrode, and end conditions at the electrode, i.e., whether or not the end of the electrode was limited by a vertical wall.

The passage of electrical current through a horizontal electrode cell, in which the lower electrode is the cathode, will result in the movement of mass by three separate and distinct mechanisms: 1. migration, 2. diffusion, and 3. natural convection.

Migration is the movement of ions under the influence of an electric field. Diffusion is the movement of mass under the influence of concentration gradients. Natural convection is the movement of fluid elements under the influence of density gradients. Natural convection may be of either the cellular or turbulent type as was found in heat transfer experiments described previously. There should be a stability criterion for each type of motion, similar to that in the heat transfer case, but the determination of these was not the object of this work.

With this picture of ionic transfer through the solution, the concept of a limiting current is easily built up. If the voltage between the electrodes in a cell is increased, the current will also increase. However, the solution is limited in its ability to provide ions to the electrode. When the concentration of reacting ions at the surface of the electrode reaches zero, no further increase in current is possible unless a new reaction takes place. The current at this point is known as the limiting current.[16] Limiting current density is the maximum rate of electrical current passage per unit area of electrode which can be utilized for a particular electrode reaction. For this work, then, limiting current density is the milliamperes per square centimeter passing through the solution which will reduce the concentration of copper ions at the surface of the cathode to zero.

The problem, then, is to measure the concentration of copper ions at the surface of the electrode. If the physical situation at the cathode is examined, it is seen that there exists essentially a concentration cell. If an electrode were placed in the cell in a region of bulk concentration, the potential measured between this reference cell and the cathode would be the potential of a concentration cell existing between the two concentration limits. This concentration cell effect at the surface of a working electrode is known as concentration polarization. The concentration polarization is given by the equation:

$$\Delta E = (RT/nF) \ln (a_o/a_i) \approx (RT/nF) \ln (C_o/C_i) \qquad (9)$$

Actually placing a reference electrode in the bulk of the solution has several drawbacks: first, the electrode would disturb the flow patterns, and second, since the solution does have a finite electrical resistance, an I · R drop would also be included in the measured potential difference. To overcome these difficulties, the reference electrode is placed in a side chamber connected to the cell as close as possible to the surface of the cathode. This side chamber is filled with fluid of bulk concentration, and the reference electrode is made of the same material as the cathode.

Two minor points interfere with the measurement of concentration at the interface in the method outlined above. Besides measuring concentration polarization, chemical polarization is measured simultaneously. However, in the measurement of limiting current, the actual value of electrode polarization* is of no consequence, rather one has to obtain the value of current at which the rate of increase of potential with current approaches infinity. The other point is that in the measurement and recording of polarization, it is necessary to draw some current through the reference electrode which results in an I · R drop and in a concentration change at the surface of the reference electrode. The measuring curcuit used in this case was designed to draw not more than 1 microampere through the reference cell. With such a small current these effects become negligible.

In order to determine the limiting current density, one has to plot the electrical current as a function of concentration polarization. Figure 3 is an actual example of a well defined limiting current curve. The dotted extension is the theoretical curve in the absence of successive electrode reactions; the actual curve bends up again, however, as a result of the decomposition of water at higher voltages. The limiting current is the actual magnitude of the current passing through the cell at the point where the rate of change of current with concentration polarization is equal to zero.

---

* For a more detailed discussion of polarization and its measurements see Eisenberg.[17]

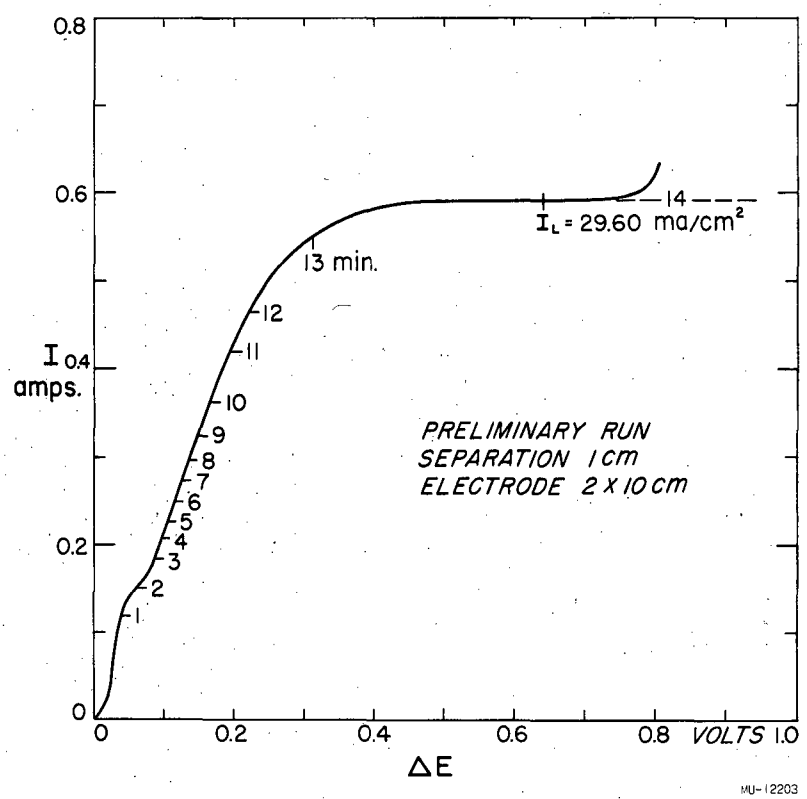

Fig. 3. A limiting current curve, - electric current as a function of polarization voltage.

Figure 4 is a schematic diagram of the experimental circuit used in the work. A Leeds and Northrup X-Y function plotter was used to directly obtain limiting current curves. Another Leeds and Northrup recorder was used to measure the change of concentration polarization with time.

Experimental Apparatus and Proceedure

The electrolytic cell used in this work was so designed as to provide the possibility of wide variations in the ranges of experimental variables and still be easy to change from one set-up to another.

Figure 5 is a section drawing and an assembly picture of the cell. The four spacers, which were used to vary the free height above the electrode, were 1, 2, 4, and 8 cm. thick respectively, allowing a minimum spacing of 1, and a maximum of 16 cm. in 1 cm. intervals. The anode compartment was separated from the cathode compartment by a 1/8 inch thick acid proof ceramic diaphram* to prevent mixing of the anolyte and catholyte. The use of this diaphram was necessary to eliminate the influence of convection currents generated by the dissolving anode, and in order to allow a more dilute solution to be used in the anode compartment, thereby preventing crystalization of copper sulfate on the anode. The anode compartment was also mechanically stirred to prevent crystalization.

One electrode of each size used is shown in figure 6.** The cathode holder, shown in figure 7, was designed to hold each different size electrode in such a manner that its surface was in the plane of the surface of the lucite blocks on either side. Lucite blocks were also used for the study of the effect of completely surrounding an electrode with walls. Figure 7 shows how these blocks were employed. These blocks were always used in identical pairs.

Figure 8 is a top view of the tank with the cathode holder in place. This picture shows how electrical contact is made to the cathode

---

* The trade name for the diaphram was "Filtros 35", obtained from Filtros, Inc., East Rochester, N. Y.

** The electrodes were 0.1, 0.2, 0.5, 1, 2, 5, 10, 20, and 30 by 10 cm.

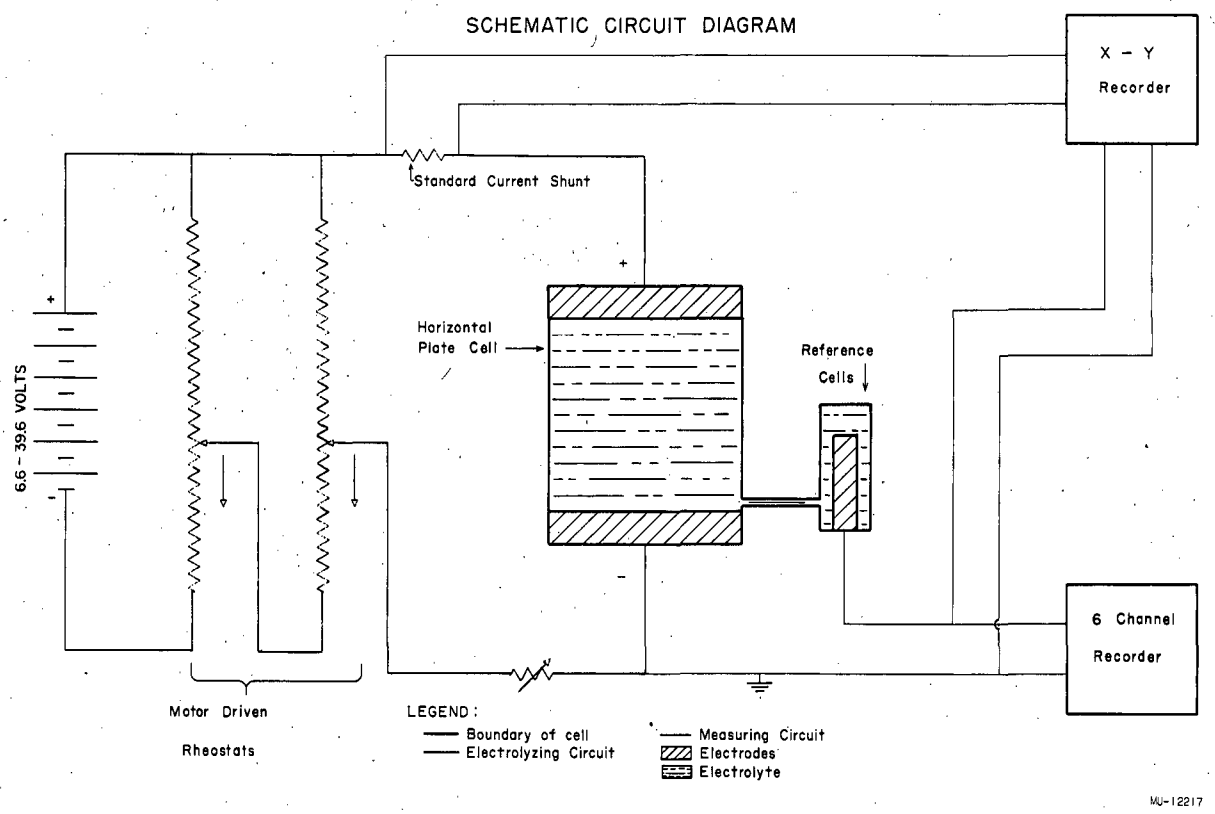

Fig. 4. Schematic diagram of experimental circuit.

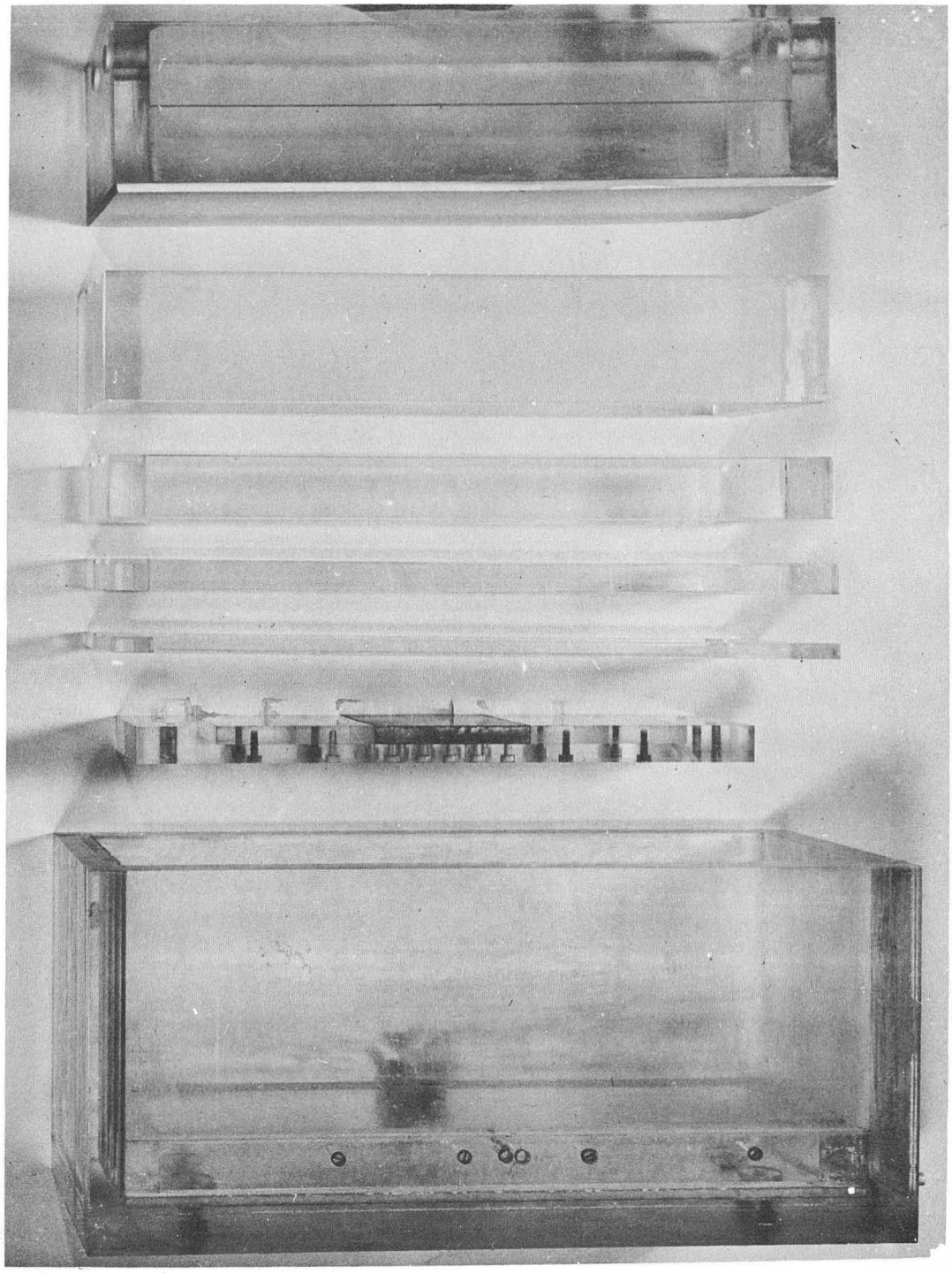

ZN-1650

Fig. 5a. Assembly photograph of experimental cell.

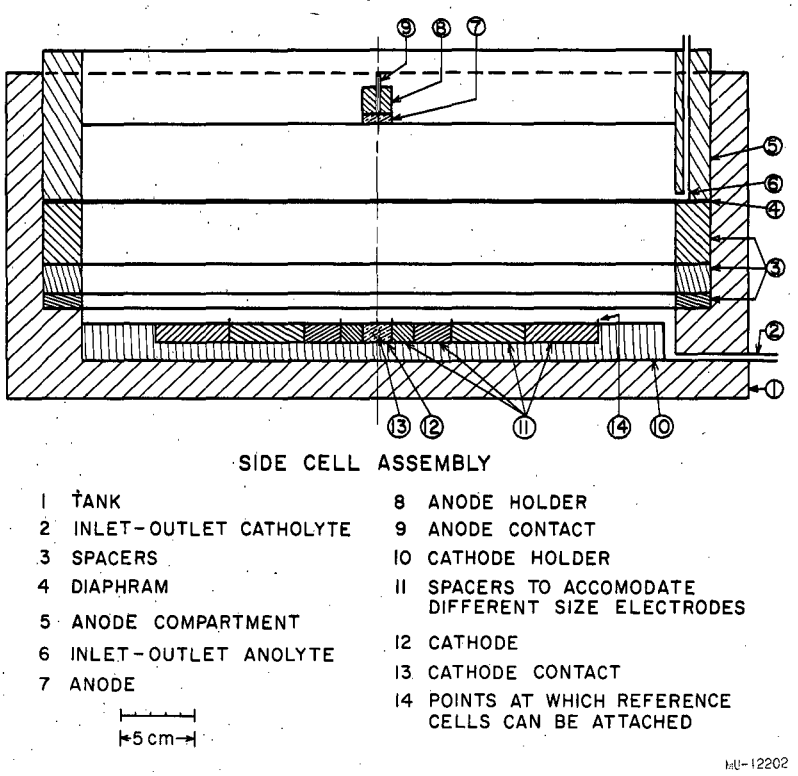

Fig. 5b. Section drawing of experimental cell.

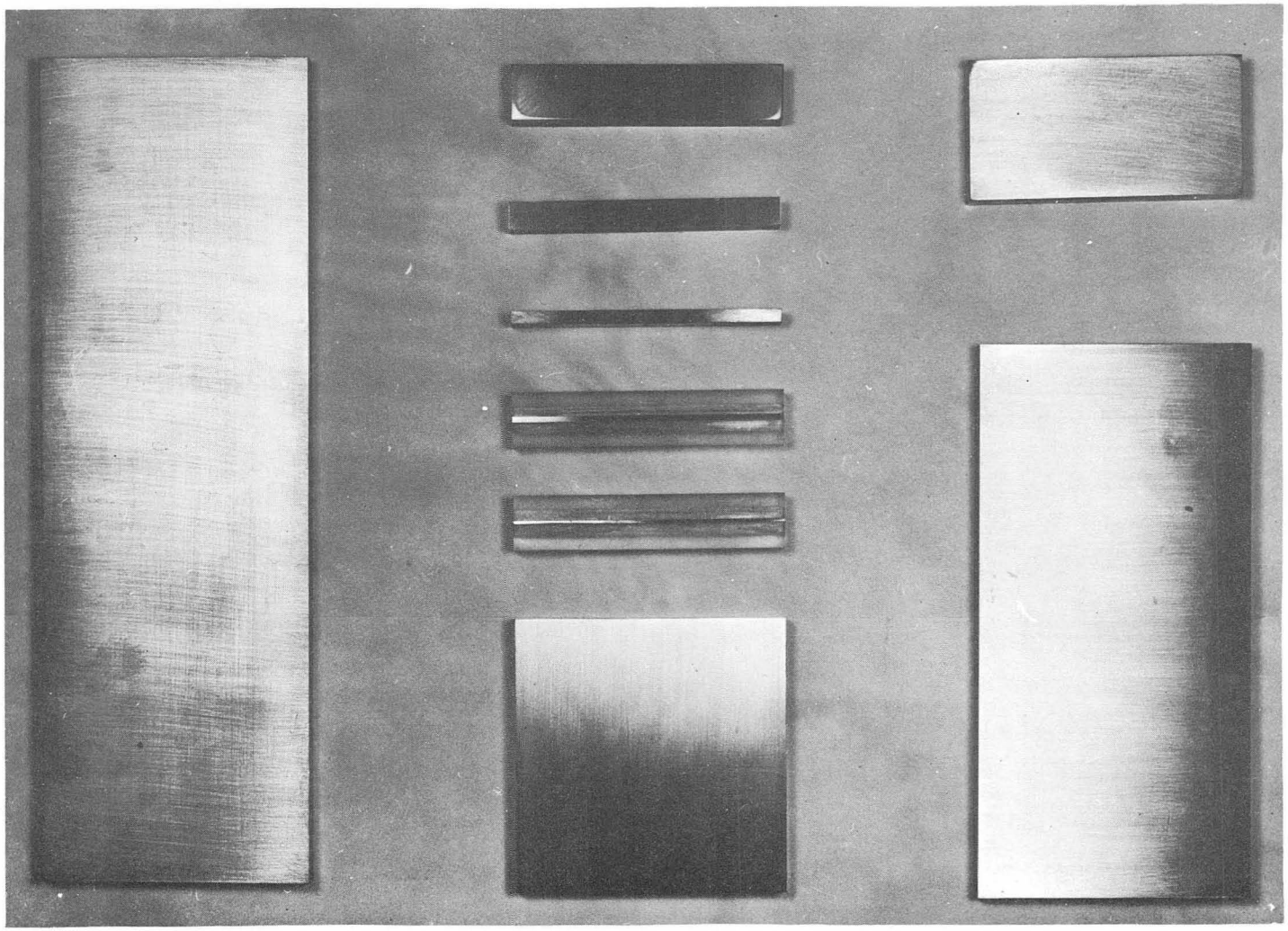

ZN-1648

Fig. 6. Example of each size electrode used.

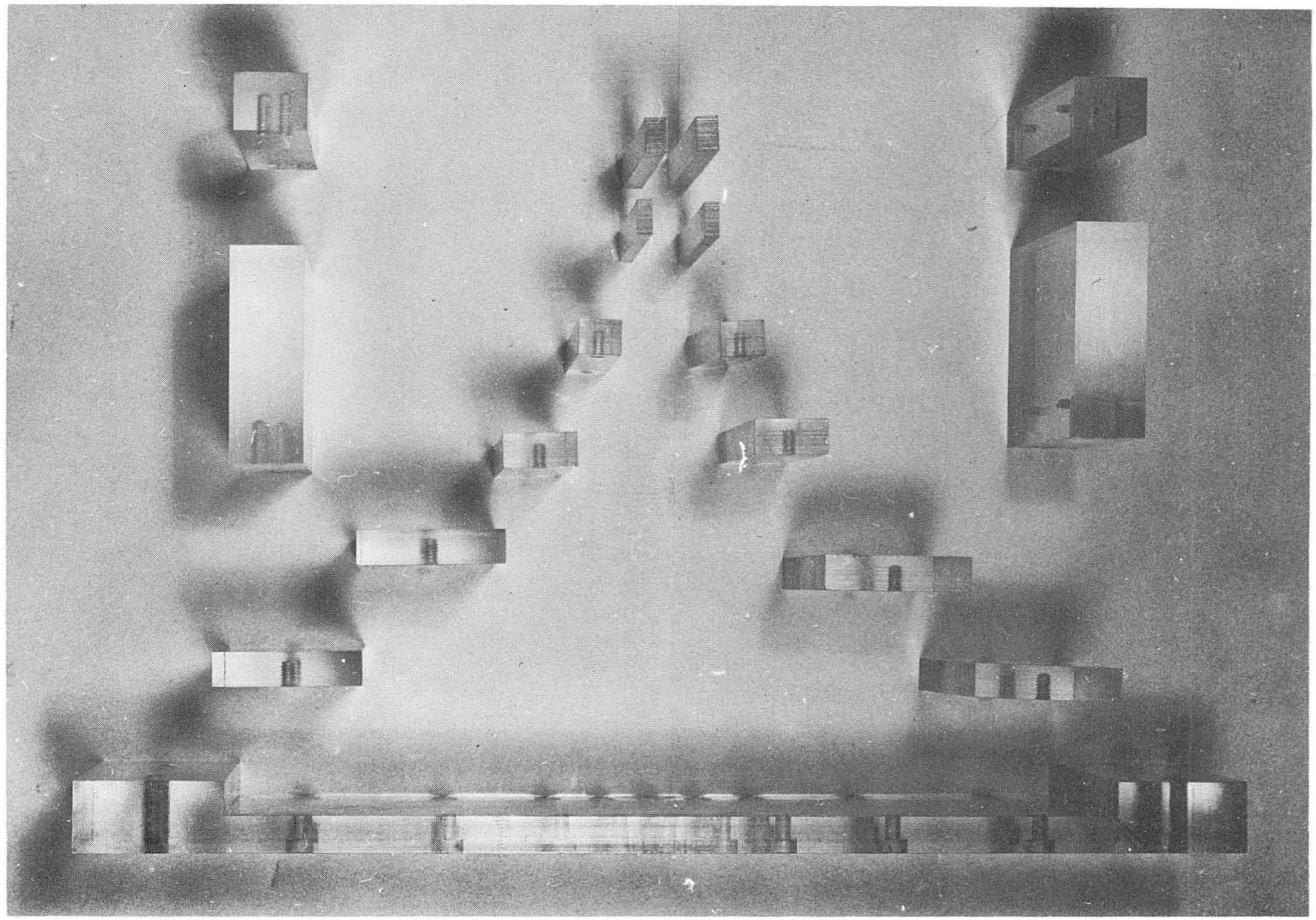

ZN-1647

Fig. 7a. Cathode holder, in which each size electrode could be flush mounted.

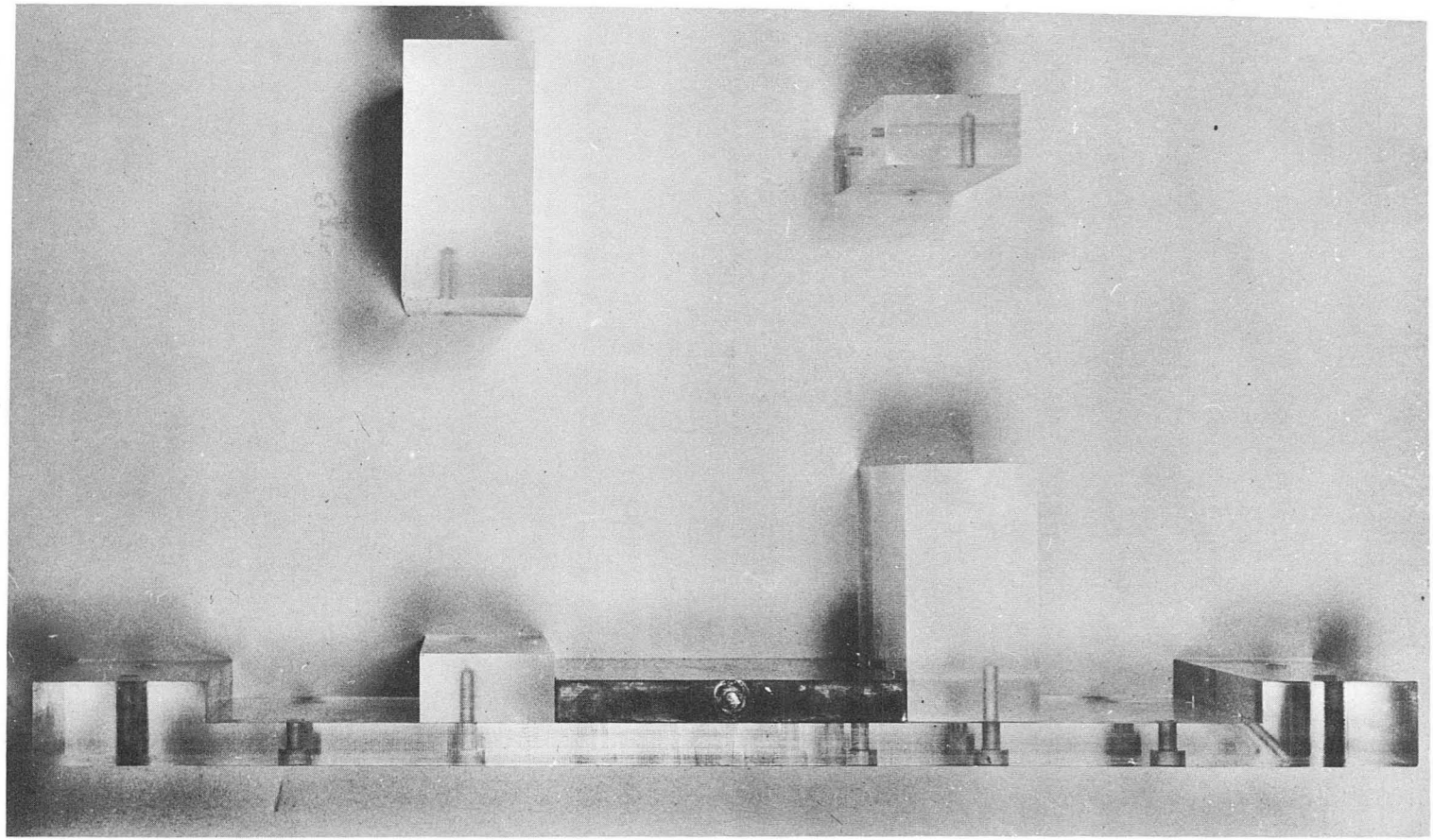

ZN-1652

Fig. 7b. Cathode holder, showing two sizes end blocks in place.

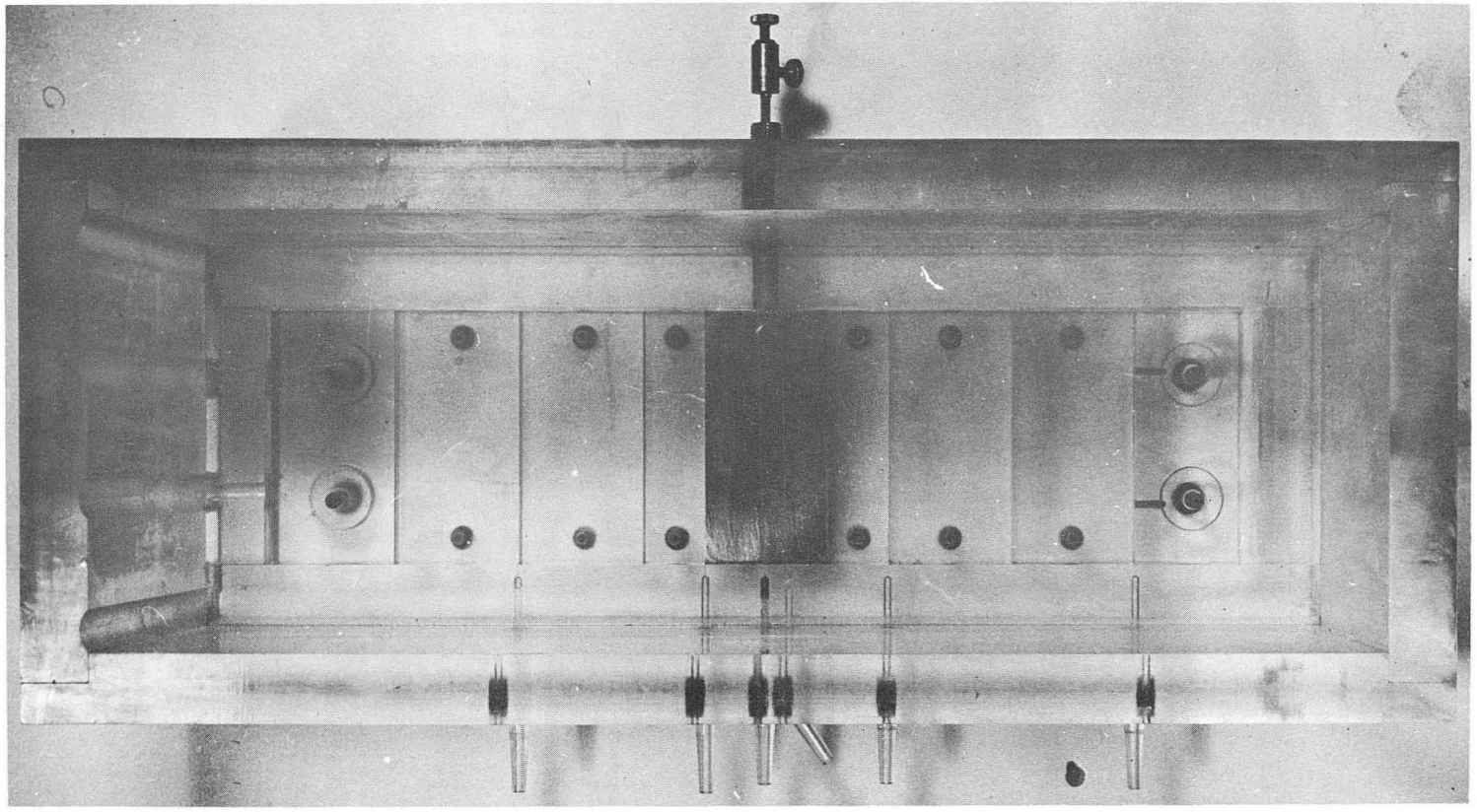

ZN-1651

Fig. 8. Top view of cathode in place, showing cathode contact and points at which reference cells could be attached.

through the side of the cell, and where reference cells could be attached. Capillary holes (13-1/2 mils in dia.) at which reference cells could be attached were located at the edge of every electrode size, and at the exact center of the electrodes. For electrodes narrower than 1 cm. no side attachment was provided because of the obvious space limitations. The unit which was attached to these holes is shown in figure 9.

Figure 10 shows the completely assembled cell. In order to minimize the influence of external vibration, all measuring equipment was placed on another table. The stirrers for the anode compartment were mounted directly to the wall and were in no way dependent on either the table or cell for support. Figure 11 shows the general experimental area. The solutions used in this work were made from the most pure chemicals* commercially available and distilled water.

During the course of the experimental work, solutions were stored in glass containers (upper left in figure 11). The catholyte was mixed to uniformity by a magnetic mixer and fed to the tank by gravity. After an experiment the catholyte would be drained into one of the glass jars under the table. Each time the supply was exhausted, the used solution was lifted by vacuum into the upper jar, mixed thoroughly, analyzed, and re-used. Determination of the copper was by the thiosulfate method,[18] of acid by a pH titration with standard NaOH, and of glycerol by a cerate oxidation.[19] In order to insure a reproducible surface quality (degree of roughness) from one electrode to another, the electrodes were machined from an oxygen-hydrogen free electrolytic copper plate, and each electrode was polished just before use with number 400 Wetordry Emery Paper. After polishing, the electrodes were washed with distilled water and degreased with acetone. Reference electrodes were prepared in the same manner. Electrodes were used immediately after preparation.

---

* Anhydrous copper sulfate, "Baker Analyzed", was obtained from the Baker Company. C. P. grade sulfuric acid and glycerol came from General Chemical Division of the Allied Chemical and Dye Corporation. For a statement of impurities see Appendix 3.

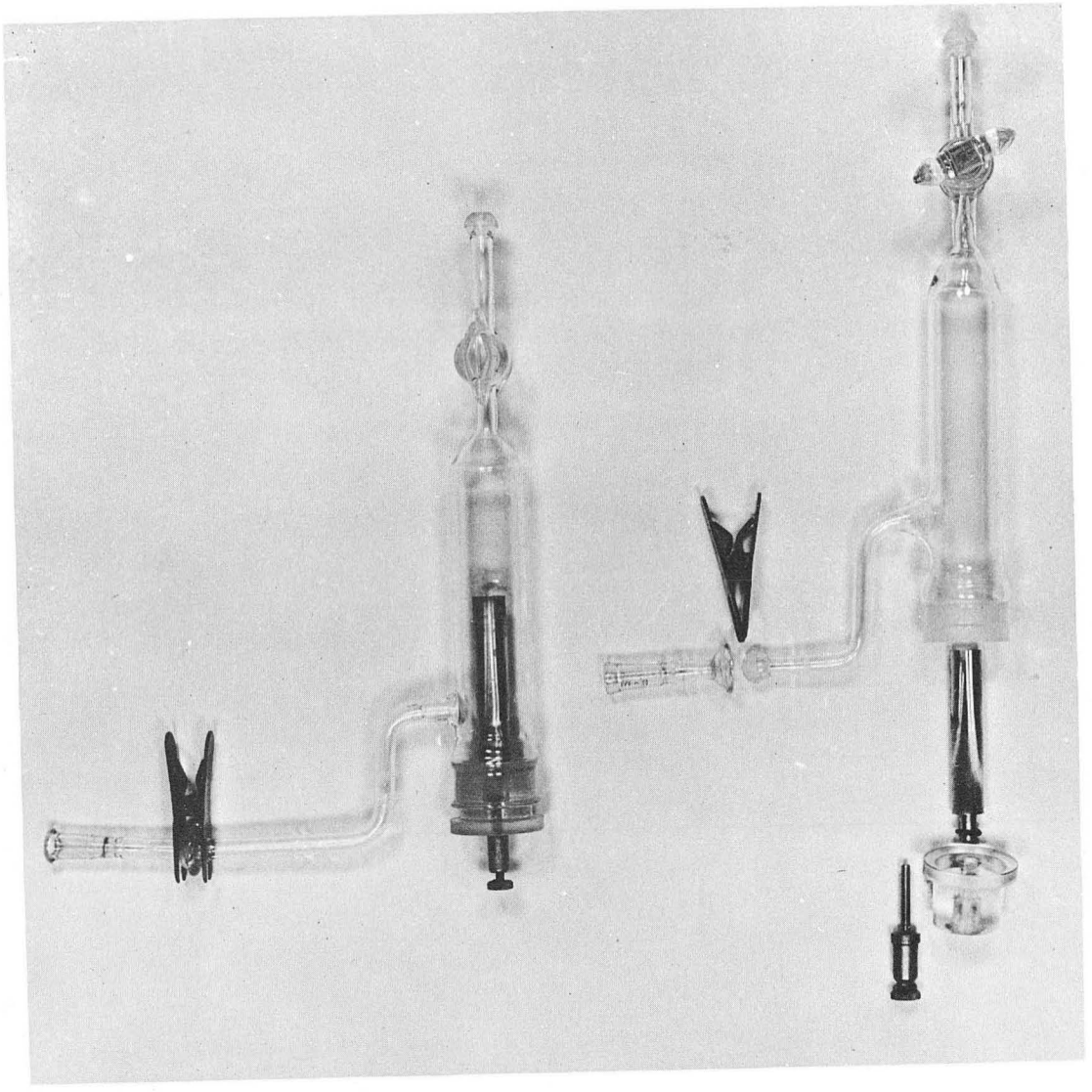

ZN-1645

Fig. 9. Reference electrodes.

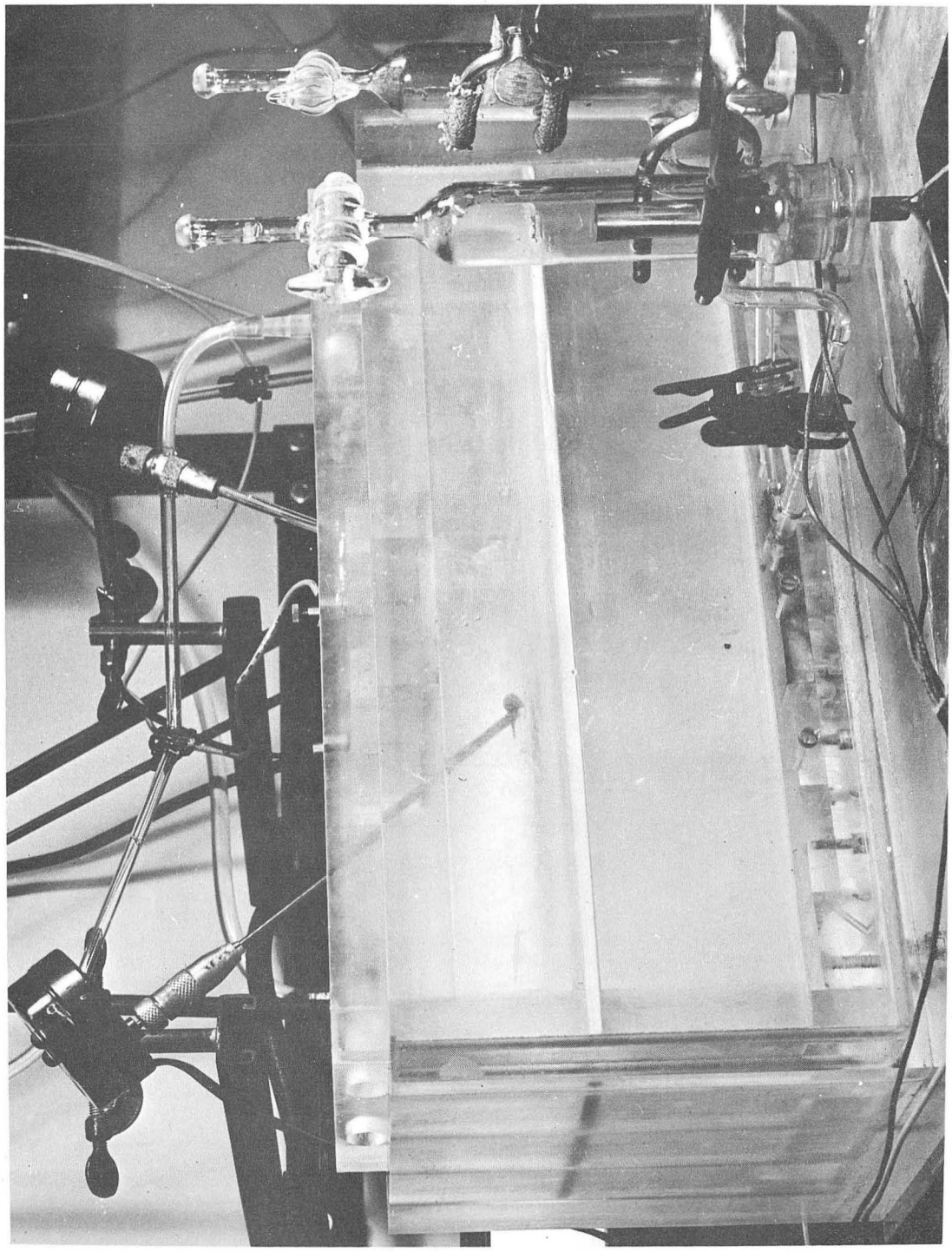

ZN-1646

Fig. 10. Assembled cell.

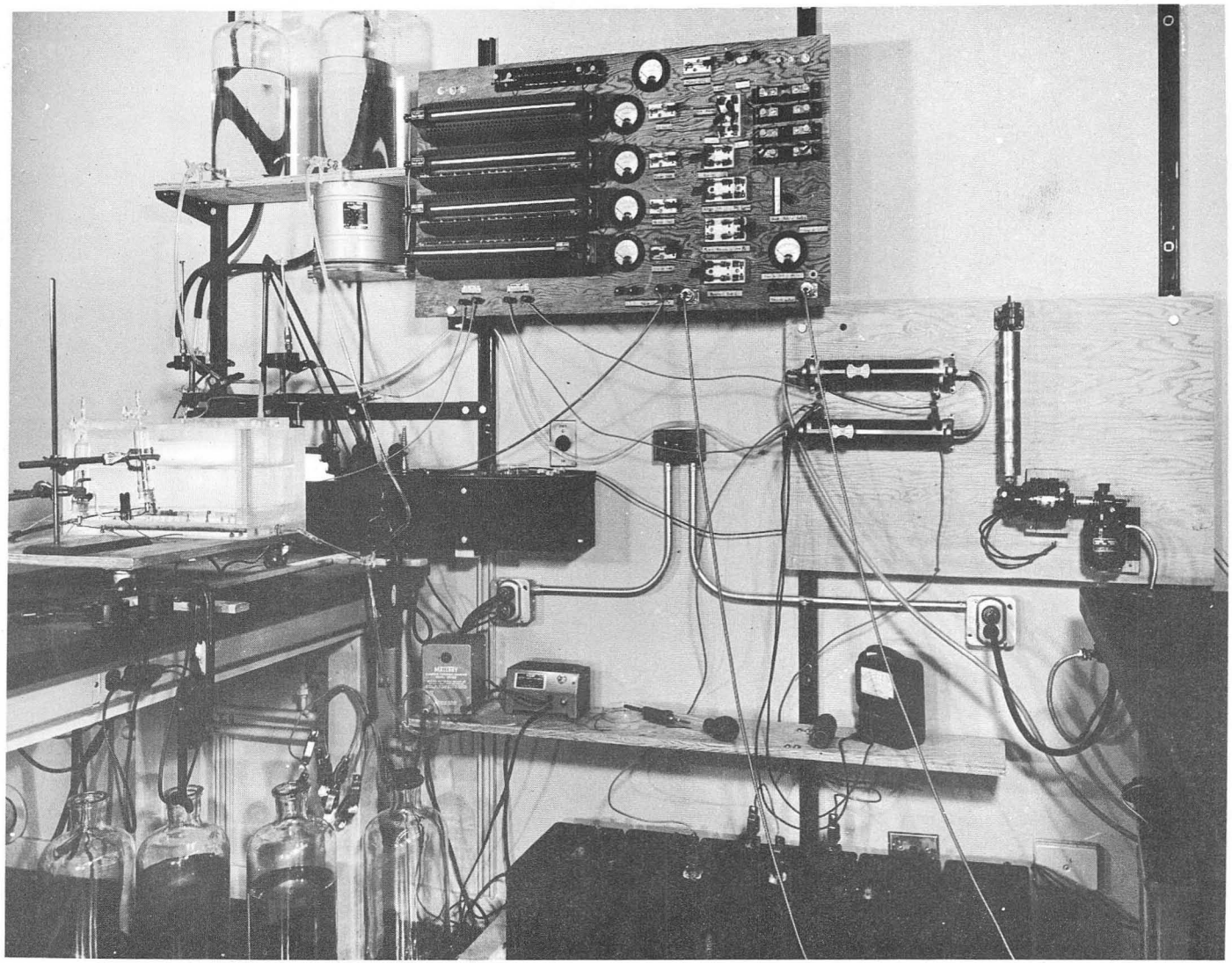

ZN-1649

Fig. 11. General view of experimental area.

In the following, the step by step proceedure of an experimental run is outlined:

1. The reference electrodes to be used were polished, washed and put in place.

2. The experimental electrode was prepared, mounted in the cathode holder, and placed in the cell.

3. Proper spacers for the run were placed in the tank and the anode compartment put in the tank.

4. The cathode chamber was filled from its supply with care so that no bubbles should be entrapped in the lower compartment.

5. The anode was placed in position, and the anode compartment filled.

6. Electrical contact was made to all electrodes, and checks made for open circuits.

7. Proper ranges for the run were selected for each recorder.

8. Voltages necessary for the run were selected from the lead storage batteries, and the motor driven rheostates set in motion.

9. At time equal zero, current was switched on and recording of experimental variables started.

10. After limiting current was exceeded, as noted on the X-Y function plotter, current was switched off, recording stopped, and cell emptied, and disassembled.

The correct choice of the length of time of a run presented an interesting problem. The run had to be long enough to allow the system to reach a steady state as far as convection and diffusion were concerned, but had to be short enough so that the bulk concentration was not changed to a noticeable extent.

It was desirable to minimize the change of bulk concentration by using as short a time as possible, while at the same time insuring that steady state was achieved. In order to determine the shortest possible duration of experimental runs, trial runs* were made in the following manner.

---

* These experiments were done using 0.24 M $CuSO_4$. Achievement of steady state in low concentration runs is discussed later.

A basic rate of change of voltage applied to the electrodes with time was decided on, and then used in several experiments starting at different initial voltages. Figure 12 is an example of such a set of runs. It is seen that there is no observable difference in limiting current densities in the two shorter runs in spite of a time difference of 25%. The difference in limiting current density in the longer run (Fig. 12) is attributed to a change in bulk density. On a basis of a large number of such experiments, the length of a run was held to between three and five minutes.

Whether or not the placement of reference electrides had an influence on the observed limiting current was another important consideration. To determine this, reference electrodes were placed at the center, at the edge, and at two other points along a 20 cm. electrode. During a run, then, a plot of concentration polarization as a function of time was made by a multipoint recorder. An example of such a plot is given in figure 13. Although the voltage at the edge of the electrode is somewhat different than that at other points during most of the run, during the critical limiting current time, all curves are practically identical. From these experiments it was determined that the position of the junction of the reference cell had essentially no effect on the observed limiting current value. In actual practice the reference cells were always placed exactly at the center of the electrode.

During the course of experimental work, it was found that by using reasonable care an electrode could be used several times with good reproducibility. Reasonable care included prevention of the formation of rough, powdery deposits, which forms after limiting current is reached, and prevention of the oxidation of the fresh copper plate. This new layer of copper appeared to oxidize very quickly upon exposure to air, forming a dark surface. In the course of taking quantitative data, a fresh electrode was used in each experiment.

Failure to change the electrolyte between runs led to very poor reproducibility. However, if the electrolyte were allowed to stand for several hours between runs, a valid limiting current measurement could again be made. It appears that the local concentration gradients in the solutions were eliminated during this time.

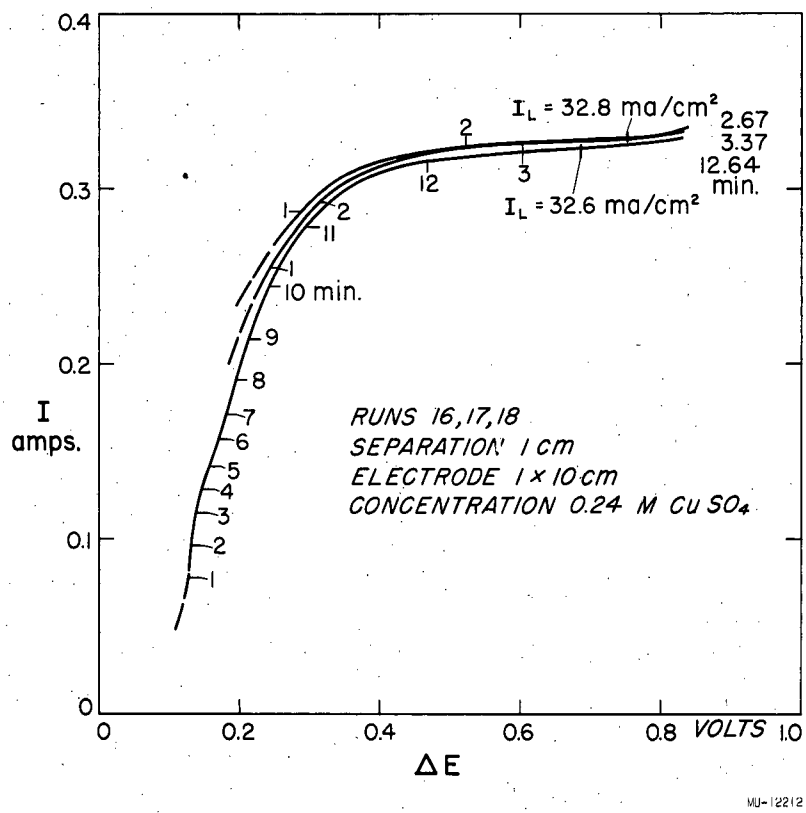

Fig. 12. Limiting current curves for different length runs with no other experimental variables changed.

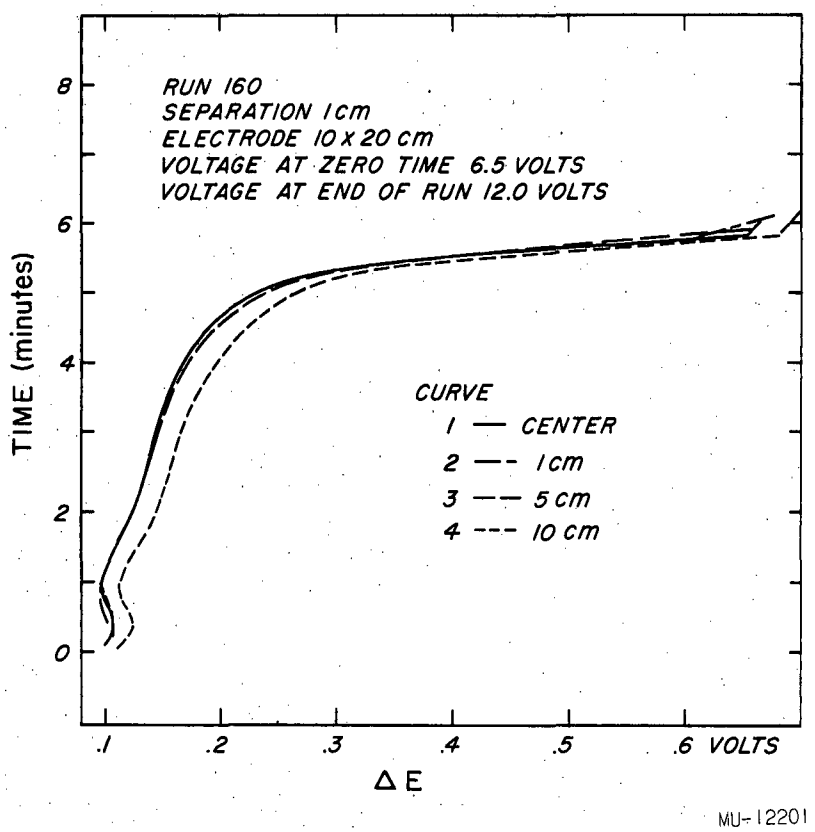

Fig. 13. Variation of polarization with time at four points along a 20 cm. electrode.

Discussion of Data

Using the standard proceedure outlined, almost 400 individual limiting current densities were measured. Approximately 100 of these were undertaken to determine the best experimental proceedure. Another 30 were measured to establish approximate limiting current ranges for particular concentrations and electrodes so that proper instrumentation could be used. Calculations were based on the final 277 experimental runs, which included 99 different experimental situations.

Figure 14 is a graph of limiting current densities as a function of free space above the electrode. The values plotted on this graph and on all following do not correspond to any individual measurements, but rather to an average value of all identical runs. From the graph it is quite obvious that concentration of the copper ion is the largest single factor in determining limiting current densities. Limiting current is shown to be a function of approximately the 4/3 power of the bulk concentration. This is not completely accurate as the properties of the liquid (viscosity, density, etc.) also vary with concentration. Table 1 gives an average value of the constant if the equation

$$I_L = b\ C_o^{4/3} \tag{10}$$

is assumed to be valid. The last item in Table 1, shows how drastically

Table 1*

Concentration	Limiting Current	"b"
0.0810 M $CuSO_4$	7.30 ma/cm^2	209.2
0.2336 "	28.10 "	195.8
0.6570 "	113.6 "	198.9
0.3706 " 5.41 M Glycerol	12.40 "	32.9

"b" changes if glycerol is added to the solution. The addition of glycerol decreases the diffusivity, and increases the viscosity and density, although the density difference between bulk and electrode surface remains

* Actual runs of average value from the group using 10 x 10 cm electrodes and 1 cm free height above the electrode.

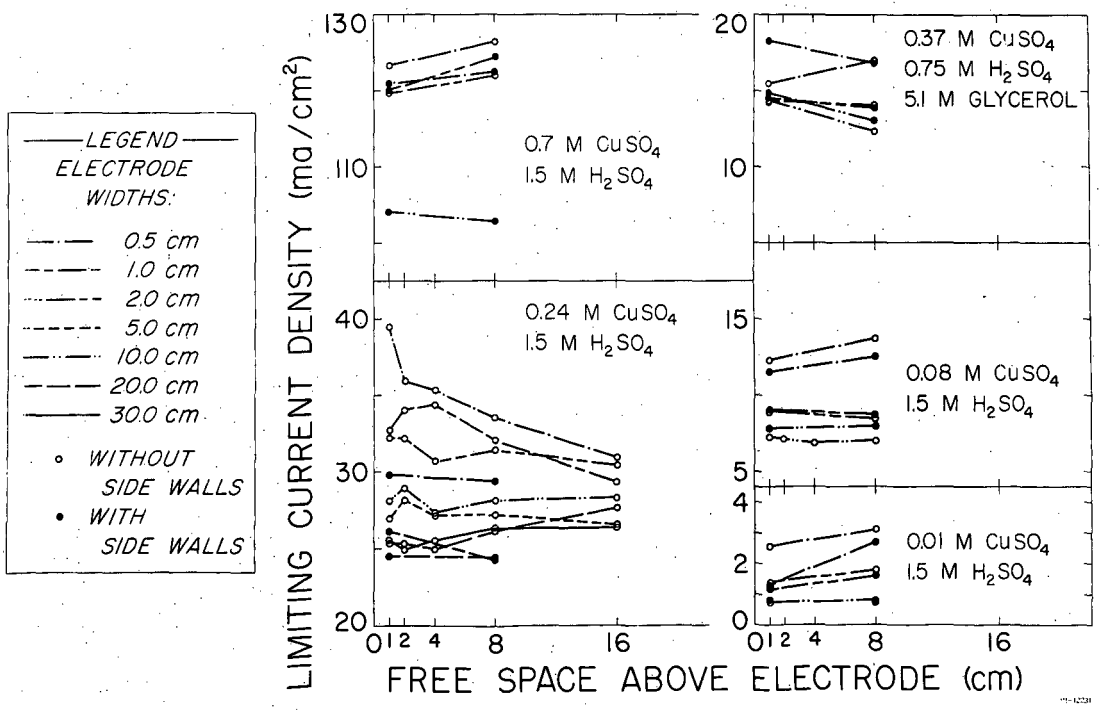

Fig. 14. Limiting current density as a function of free space above the electrode for each concentration.

almost the same as in solutions without glycerol. With large changes of liquid properties, equation 10 cannot even be used as an approximation. In figure 15, the limiting current density as a function of the width of electrode* is given. Examination of figures 14 and 15 have failed to show any general dependence of limiting current with free space above the electrode. However, analogus work in heat transfer,[11,12,13] has noted a definite dependence on this parameter. It is expected that the dependence should be very sharp below a certain critical distance, and extremely weak above this critical distance. In the case of heat transfer, the distances studied were on the order of 1 cm. and less, while in this work the smallest distance examined was 1 cm. Distances smaller than 1 cm. are seldom used in electrolytic cells.

On the other hand, a significant difference in limiting current densities was observed with a change in width of electrode, as shown in figure 15. Due to the possibility of increased horizontal transfer of ions at the edge of the electrode, it is expected that the local mass transfer coefficient at that point would be higher than that at the center. The importance of such an edge effect decreases as the width of the electrode becomes larger, until, for the electrodes over 2 cm. wide** it is shown to be negligible. If this horizontal supply of ions were shut off by placing walls at the edge of the electrode, it could be expected that the limiting current density would fall to, or even below that for larger electrodes with free ends. While it is a fact that on smaller electrodes the limiting current density is significantly lowered, in general, it is not lowered to the predicted value. For example, using 0.24 M $CuSO_4$, the limiting current density for a 0.1 cm. wide electrode dropped from 52-1/2 to 48-1/2 ma/cm^2 when end walls were added, while the average value for large electrodes in the same concentration was about 26 ma/cm^2. This points out that there is some other, as yet unidentified mechanism at work.

---

* One dimension of all electrodes is 10 cm.

** Experimental results, see Figure 15.

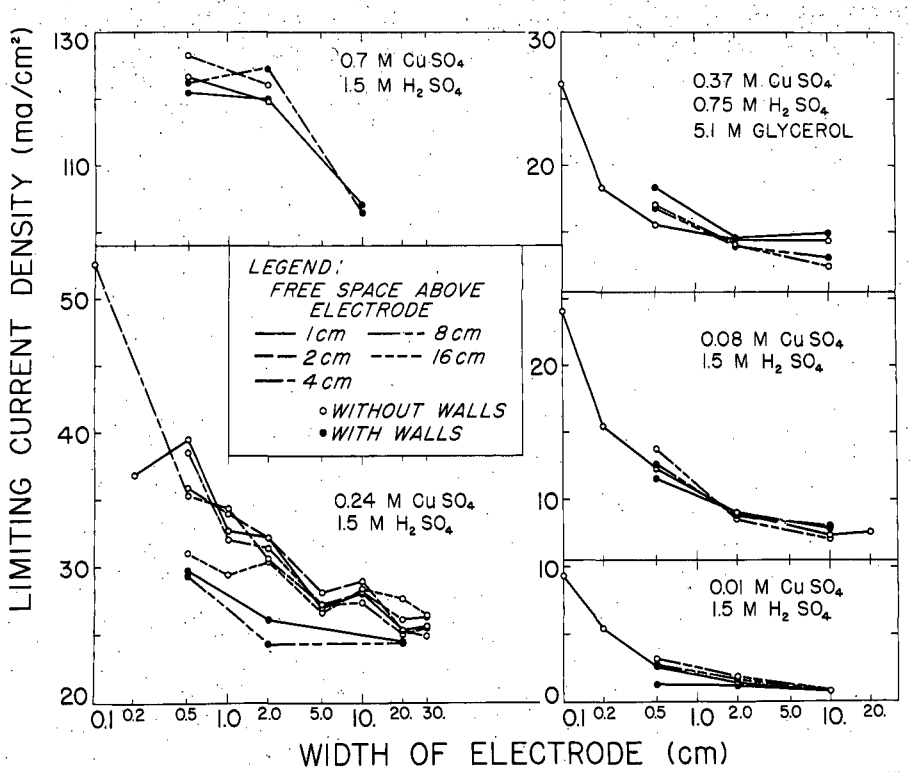

Fig. 15. Limiting current density as a function of width of electrode for each concentration.

In this work reproducibility was measured by percent deviation.* For the 277 calculated runs, the average percent deviation was 4.7%. The average percent deviation for each concentration is given in Table 2.

Table 2

Concentration	Average Deviation	No. of Runs Considered
0.01 M $CuSO_4$	22.1%	41
0.08 "	8.4%	50
0.24 "	1.3%	125
0.69 "	0.4%	26
0.37 " 5.41 M Glycerol	2.6%	35
Overall	4.7%	277

Within each concentration group, the deviation for the smaller electrodes was higher than average, and the deviation for the higher electrodes, lower.

Reproducibility, as poor as that exhibited by 0.01 M $CuSO_4$, reflects considerable doubt on the measurements made in that group. In figure 16, a typical limiting current for a 0.01 M $CuSO_4$ run is reproduced. This concentration is the only one to show this characteristic dip of the I_L versus E curve.

Examination of the concentration polarization-time curves point to another peculiarity of the 0.01 M $CuSO_4$ runs. A normal plot, presented in figure 13, shows that the rate of change of voltage with time is extremely low until close to limiting current. At this time the change of concentration polarization is very rapid. In contrast to this, is the graph shown in figure 17, in which the rate of change of polarization voltage with time is much more constant throughout the entire experimental run. The obvious interence is that the build up

* Percent Deviation =

$$\frac{(I_L \text{ Run} - I_L \text{ Av. for identical runs})}{I_L \text{ Av. for identical runs}}$$

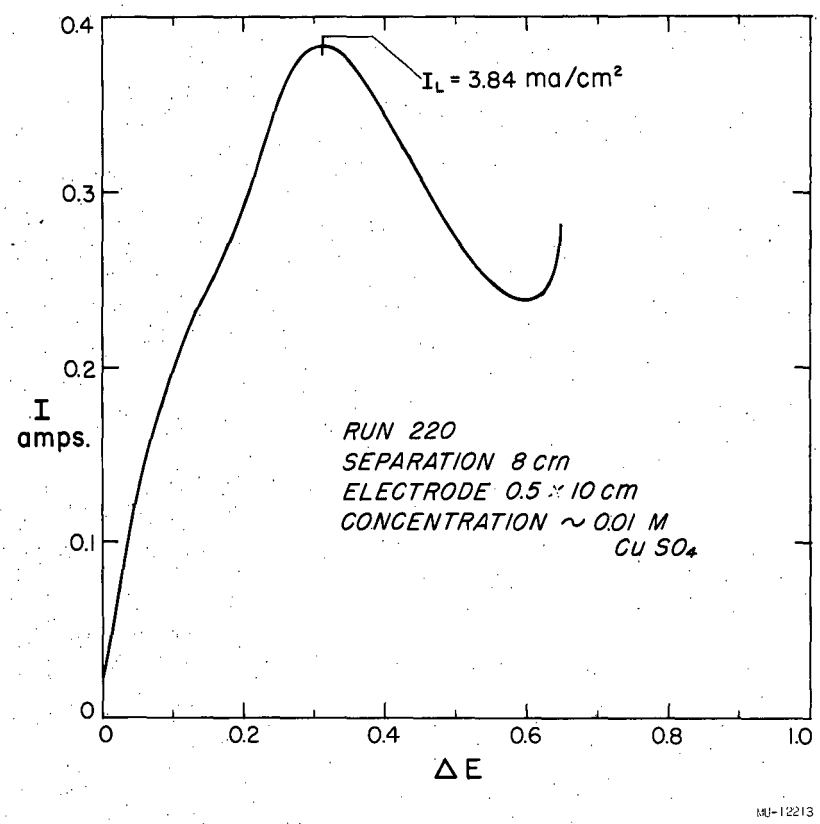

Fig. 16. Typical limiting current curve for 0.01 M $CuSO_4$ concentration.

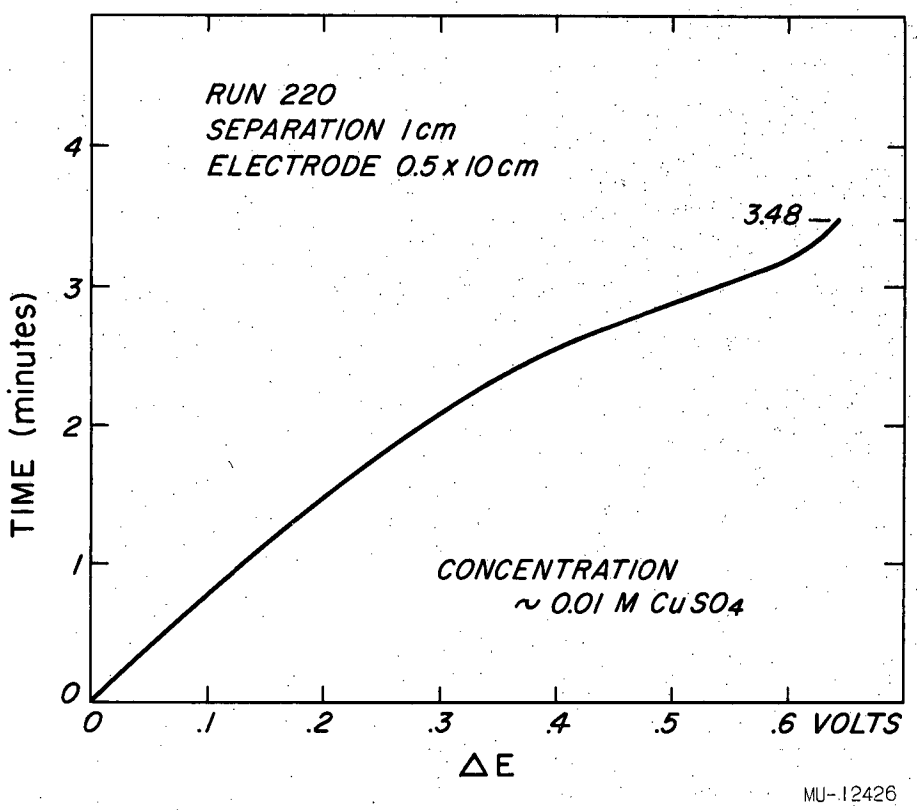

Fig. 17. Typical variation of polarization with time for 0.01 M $CuSO_4$ concentration.

of the convectional transfer process is so slow that one cannot observe a typical steady state plateau corresponding to a true limiting current. Unsteady state diffusion is the mode of mass transfer in the initial period, and since the supply of ions very close to the electrode surface is high at the beginning of a run, the current rises quickly to a large value. This supply is rapidly depleted and the current drops with time in spite of the increasing applied voltage. At this point, free convection begins, but the driving force (density difference) is small and convection develops slowly. Before the free convection has time to develop fully and reach steady state, the voltage across the cell reaches the value sufficient to start the decomposition of water.

The obvious solution to this problem would be simply to lengthen the time of the runs. In the case of dilute solutions, the resultant change in bulk concentration above the electrode would be so high that the interpretation of limiting current values thus obtained would be impossible.

Additional evidence supporting the phenomena just described is presented in table 3. Drastic differences in limiting current densities are produced in runs of different duration. Data are also presented for 0.08 M $CuSO_4$ runs, in which it is seen that the effect is present, but is much less noticeable. At still higher concentrations the measured value of limiting current was essentially independent of the time elapsed until the limiting current was reached.*

Table 3

Concentration	Electrode Width	Length of Run	Limiting Current Density
0.0129 M $CuSO_4$	0.5 cm.	3.50 min.	2.80 ma/cm^2
0.0129 "	0.5 cm.	2.66 min.	3.40 "
0.0110 "	10.0 cm.	5.50 min.	0.72 "
0.0110 "	10.0 cm.	3.00 min.	0.82 "
0.0782 "	0.5 cm.	4.75 min.	12.4 "
0.0782 "	0.5 cm.	3.64 min.	12.7 "
0.0800 "	10.0 cm.	5.17 min.	6.90 "
0.0800 "	10.0 cm.	2.72 min.	7.22 "

* If shorter than 5 min.

Correlation of Data

On the basis of theoretical work done recently by Levy,[15] and also because heat transfer data obtained under free convection conditions at horizontal plates could be successfully correlated by the use of the dimensionless equation

$$Nu = a\ (Pr\ Gr)^c,$$

correlation of data obtained in this work was attempted using the form

$$Nu' = a\ (Sc\ Gr)^c \qquad (11)$$

As in earlier heat transfer work,[11,12,13] the free space (height) above the electrode was used as the characteristic length in the Nusselt number for mass transfer and in the Grashof number. Figure 18 shows the results of correlation by equation 11.* Actually, the least square exponent in figure 18 is slightly less than 1/3 (0.326). However, since the difference was small, and theoretical considerations predict an exponant of 1/3, this latter value was employed. In this case, then, least square treatment provides the equation

$$Nu' = 0.179\ (Sc\ Gr)^{1/3} \qquad (12)$$

Examination of this equation for dependence on the characteristic dimension, reveals that it cancels out, making its choice of no importance.

Table 4 gives an example of each of the different experimental situations, the physical properties of the liquid in that run, and the value of the dimensionless groups. Examination of this table will provide the complete range of all physical variables studied.

In line with what was said concerning the accuracy of the 0.01 M $CuSO_4$ runs, figure 19 shows the relationship of the calculated points and equation 12. In establishing the correlation (equation 12) the data obtained on the 0.01 M $CuSO_4$ solutions were not considered, since it is very doubtful whether in any of these runs a true value of the limiting current could be evaluated.

The dependence of width of electrode is shown in figure 15. An attempt to isolate this dependence is given in figure 20, where the least square lines from equation 11 with a 1/3 exponent are plotted for each electrode size.** Table 5 lists the calculated intercepts for each

* For a discussion of calculations see Appendix 1.

** In order not to be too confusing, only points from the 0.24 M $CuSO_4$ concentration are shown in figure 20.

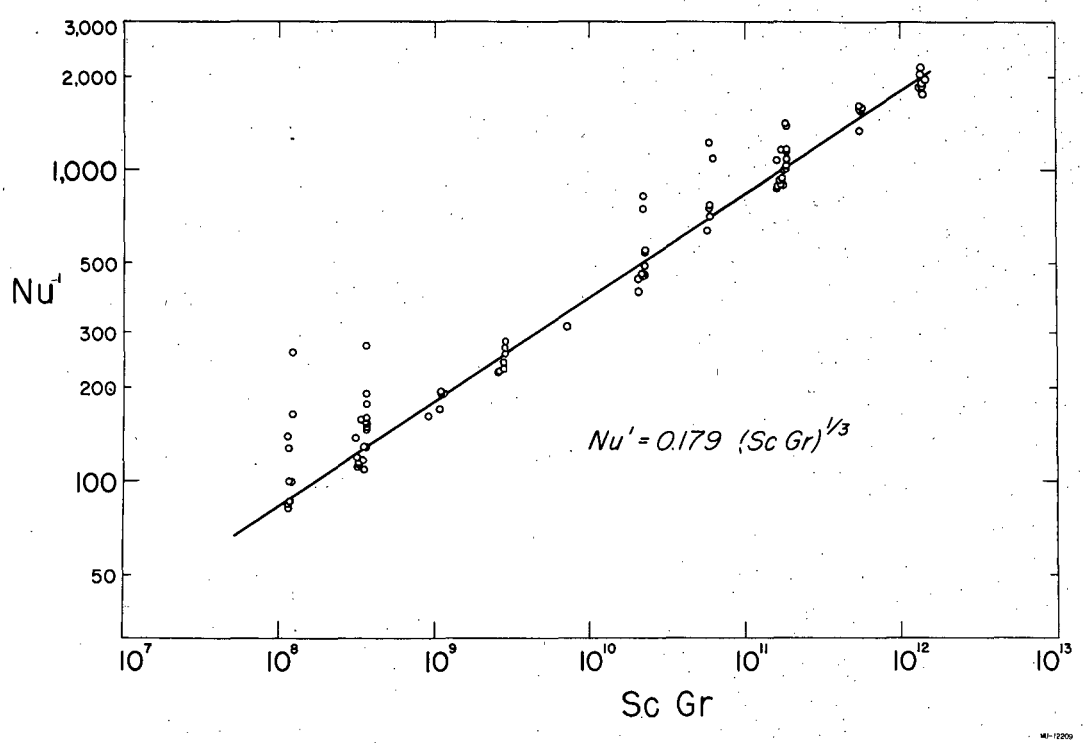

Fig. 18. General correlation, with free space above the electrode as characteristic dimension.

Run No.	Electrode Width mm	Free Height cm	$CuSO_4$ molarity	H_2SO_4 molarity	ΔC H_2SO_4 moles/liter	Limiting Current Density - ma/cm^2	Mass Transfer Coefficient x 10^3 - cm/sec	Average Viscosity centipoise	Bulk Density gm/cm^2	$\Delta\rho$ gm/cm^3	Average Diffusion Coefficient x 10^5 cm^2/sec	Transference No. $CuSO_4$ x 10^3	Nu'	Sc	Gr
229	1	1	0.0140	1.724	0.0057	5.35	1.9728	1.356	1.113	0.0014	0.549	0.06	359	2236	8597
225	2	1	0.0140	1.724	0.0057	4.09	1.5082	1.356	2.113	0.0014	0.549	0.06	274	2236	8597
216	5	1	0.0135	1.678	0.0055	1.52	0.5811	1.342	3.113	0.0014	0.555	0.06	104	2195	8462
209	5*	1	0.0133	1.662	0.0054	1.00	0.3875	1.337	3.123	0.0013	0.557	0.06	69	2181	8337
202	20	1	0.0132	1.645	0.0054	1.23	0.4816	1.332	5.113	0.0013	0.559	0.06	86	2166	8335
204	20*	1	0.0132	1.645	0.0054	1.09	0.4268	1.332	5.123	0.0013	0.559	0.06	76	2166	8335
183	100	1	0.0110	1.570	0.0045	0.82	0.3862	1.308	7.112	0.0011	0.568	0.06	67	2100	7218
187	100*	1	0.0110	1.570	0.0045	0.80	0.3768	1.308	7.122	0.0011	0.568	0.06	66	2100	7218
218	5	8	0.0136	1.691	0.0056	2.72	1.0293	1.346	3.413	0.0014	0.553	0.06	1488	2206	4370595
221	5*	8	0.0139	1.711	0.0056	1.98	0.7380	1.352	3.423	0.0014	0.550	0.06	1071	2225	4395253
192	20	8	0.0122	1.605	0.0050	1.60	0.6794	1.319	5.412	0.0012	0.564	0.06	963	2130	3990722
190	20*	8	0.0113	1.580	0.0046	1.25	0.5731	1.311	5.422	0.0011	0.567	0.06	807	2109	3776593
189	100	8	0.0113	1.580	0.0046	0.82	0.3759	1.311	7.412	0.0011	0.567	0.06	529	2109	3776696
188	100*	8	0.0113	1.580	0.0046	0.79	0.3622	1.311	7.422	0.0011	0.567	0.06	510	2109	3776696
176	1	1	0.0860	1.580	0.0347	22.50	1.3550	1.337	1.112	0.0090	0.557	0.43	243	2177	55037
179	2	1	0.0860	1.580	0.0347	18.40	1.1080	1.337	2.112	0.0090	0.557	0.43	198	2177	55037
143	5	1	0.0782	1.450	0.0319	12.10	0.8013	1.296	3.112	0.0081	0.574	0.44	139	2064	52465
149	5*	1	0.0790	1.460	0.0322	10.70	0.7014	1.299	3.122	0.0082	0.573	0.45	122	2073	52819
161	20	1	0.0820	1.490	0.0333	8.99	0.5677	1.309	5.112	0.0086	0.568	0.45	99	2099	54153
164	20*	1	0.0830	1.510	0.0337	9.03	0.5634	1.315	5.122	0.0087	0.566	0.45	99	2116	54521
157	100	1	0.0810	1.470	0.0330	7.38	0.4718	1.302	7.112	0.0085	0.571	0.45	82	2082	54030
165	100*	1	0.0830	1.510	0.0337	7.81	0.4873	1.315	7.122	0.0087	0.566	0.45	86	2116	54522
160	200	1	0.0810	1.470	0.0330	7.56	0.4833	1.302	8.112	0.0085	0.571	0.45	84	2082	54030
159	100	2	0.0810	1.470	0.0330	7.10	0.4539	1.302	7.212	0.0085	0.571	0.45	158	2082	432246
154	100	4	0.0800	1.470	0.0326	6.90	0.4466	1.302	7.312	0.0084	0.571	0.45	312	2081	3414611

Table 4

ZN-1641

Run No.	Electrode Width mm	Free Height cm	$CuSO_4$ molarity	H_2SO_4 molarity	ΔC H_2SO_4 moles/liter	Limiting Current Density - ma/cm^2	Mass Transfer Coefficient x 10^3 - cm/sec	Average Viscosity centipoise	Bulk Density gm/cm^2	$\Delta \rho$ gm/cm^3	Average Diffusion Coefficient x 10^5 cm^2/sec	Transference No. $CuSO_4$ x 10^3	Nu'	Sc	Gr
150	5	8	0.0790	1.460	0.0322	14.40	0.9440	1.299	3.412	0.0082	0.573	0.45	1317	2073	27043348
178	5*	8	0.0860	1.580	0.0347	12.60	0.7588	1.337	3.422	0.0090	0.557	0.43	1089	2177	28180520
162	20	8	0.0820	1.490	0.0333	8.50	0.5368	1.309	5.412	0.0086	0.568	0.45	754	2099	27726781
163	20*	8	0.0830	1.510	0.0337	8.76	0.5466	1.315	5.422	0.0087	0.566	0.45	772	2116	27915069
152	100	8	0.0800	1.470	0.0326	7.22	0.4674	1.302	7.412	0.0084	0.571	0.45	654	2081	27316889
166	100*	8	0.0830	1.540	0.0336	8.00	0.4991	1.324	7.422	0.0087	0.562	0.43	709	2141	27619840
101	2	1	0.2278	1.647	0.0874	36.20	0.8225	1.409	2.111	0.0249	0.530	1.03	155	2382	138738
1	5	1	0.2444	1.501	0.0942	39.50	0.8363	1.371	3.111	0.0267	0.544	1.29	153	2272	156180
103	5*	1	0.2136	1.693	0.0820	29.60	0.7173	1.418	3.121	0.0232	0.526	0.92	136	2408	128162
16	10	1	0.2433	1.525	0.0937	32.80	0.6976	1.378	4.111	0.0265	0.541	1.25	128	2291	154217
32	20	1	0.2408	1.536	0.0927	32.20	0.6920	1.380	5.111	0.0263	0.540	1.23	127	2298	152125
106	20*	1	0.2156	1.687	0.0828	26.20	0.6290	1.417	5.121	0.0235	0.527	0.94	119	2405	129686
45	50	1	0.2385	1.566	0.0917	27.30	0.5923	1.388	6.111	0.0260	0.537	1.18	110	2321	149176
61	100	1	0.2336	1.608	0.0897	27.90	0.6181	1.399	7.111	0.0255	0.533	1.11	115	2353	144105
71	200	1	0.2196	1.674	0.0843	25.00	0.5892	1.414	8.111	0.0239	0.528	0.97	111	2397	132616
110	200*	1	0.2168	1.683	0.0832	24.50	0.5849	1.416	8.121	0.0236	0.527	0.95	110	2403	130538
82	300	1	0.2196	1.674	0.0843	25.60	0.6034	1.414	9.111	0.0239	0.528	0.97	114	2397	132615
8	5	2	0.2438	1.525	0.0938	35.60	0.7556	1.378	3.211	0.0266	0.541	1.26	278	2292	1236198
19	10	2	0.2430	1.523	0.0936	34.00	0.7240	1.377	4.211	0.0265	0.542	1.25	267	2289	1233896
33	20	2	0.2402	1.543	0.0924	32.20	0.6937	1.382	5.211	0.0262	0.540	1.22	256	2303	1211290
49	50	2	0.2369	1.580	0.0910	27.90	0.6095	1.392	6.211	0.0258	0.536	1.15	227	2332	1179609
62	100	2	0.2336	1.608	0.0897	29.10	0.6447	1.399	7.211	0.0255	0.533	1.11	241	2353	1152840
72	200	2	0.2200	1.672	0.0845	25.10	0.5905	1.414	8.211	0.0240	0.528	0.97	223	2396	1063360
86	300	2	0.2182	1.680	0.0838	24.80	0.5883	1.416	9.211	0.0238	0.527	0.96	222	2401	1051949
266	1	4	0.2368	1.405	0.0921	53.46	1.1681	1.341	1.314	0.0257	0.556	1.37	839	2186	10030464

Table 4 (continued)

ZN-1642

Run No.	Electrode Width mm	Free Height cm	$CuSO_4$ molarity	H_2SO_4 molarity	ΔC H_2SO_4 moles/liter	Limiting Current Density - ma/cm^2	Mass Transfer Coefficient x 10^3 - cm/sec	Average Viscosity centipoise	Bulk Density gm/cm^2	$\Delta \rho$ gm/cm^3	Average Diffusion Coefficient x 10^5 cm^2/sec	Transference No. $CuSO_4$ x 10^3	Nu'	Sc	Gr
268	F*	4	0.2368	1.405	0.0921	45.36	0.9911	1.341	1.324	0.0257	0.556	1.37	712	2186	10030464
10	5	4	0.2437	1.516	0.0939	34.90	0.7410	1.375	3.311	0.0266	0.542	1.27	546	2284	9920409
23	10	4	0.2423	1.527	0.0933	34.50	0.7368	1.378	4.311	0.0264	0.541	1.25	544	2292	9829184
37	20	4	0.2397	1.551	0.0922	30.90	0.6671	1.384	5.311	0.0262	0.539	1.20	494	2310	9644560
51	50	4	0.2360	1.587	0.0907	27.20	0.5964	1.394	6.311	0.0257	0.535	1.14	445	2337	9378611
65	100	4	0.2320	1.618	0.0890	27.50	0.6134	1.402	7.311	0.0253	0.532	1.09	460	2360	9128896
74	200	4	0.2202	1.671	0.0845	25.10	0.5900	1.414	8.311	0.0240	0.528	0.97	446	2395	8516320
87	300	4	0.2182	1.680	0.0838	24.70	0.5859	1.416	9.311	0.0238	0.527	0.96	444	2401	8415596
13	5	8	0.2256	1.654	0.0866	32.20	0.7387	1.410	3.411	0.0246	0.529	1.02	1115	2386	70194380
105	5*	8	0.2144	1.691	0.0823	29.20	0.7050	1.418	3.421	0.0233	0.526	0.93	1070	2407	65959936
26	10	8	0.2415	1.540	0.0929	32.20	0.6899	1.382	4.411	0.0264	0.540	1.23	1021	2302	78040576
39	20	8	0.2391	1.559	0.0919	31.50	0.6817	1.386	5.411	0.0261	0.538	1.19	1012	2316	76764800
108	20*	8	0.2150	1.689	0.0826	24.30	0.5850	1.417	5.421	0.0234	0.527	0.93	887	2406	66165120
55	50	8	0.2347	1.597	0.0901	27.30	0.6020	1.396	6.411	0.0256	0.534	1.12	900	2344	74408345
66	100	8	0.2316	1.621	0.0889	28.20	0.6302	1.402	7.411	0.0253	0.532	1.08	946	2362	72641728
78	200	8	0.2270	1.643	0.0871	26.10	0.5951	1.407	8.411	0.0248	0.530	1.04	897	2377	70910080
113	200*	8	0.2168	1.683	0.0832	24.40	0.5825	1.416	8.421	0.0236	0.527	0.95	883	2403	66835840
91	300	8	0.2223	1.665	0.0853	26.50	0.6170	1.413	9.411	0.0242	0.528	0.99	933	2392	68910458
15	5	16	0.2251	1.656	0.0864	30.40	0.6990	1.411	3.511	0.0245	0.529	1.01	2112	2387	559631564
28	10	16	0.2240	1.659	0.0860	29.70	0.6863	1.411	4.511	0.0244	0.529	1.00	2074	2389	556519424
44	20	16	0.2385	1.566	0.0917	30.50	0.6618	1.388	5.511	0.0260	0.537	1.18	1968	2321	611010560
57	50	16	0.2340	1.605	0.0898	26.70	0.5905	1.398	6.511	0.0255	0.534	1.11	1769	2351	591740928
68	100	16	0.2307	1.628	0.0885	28.40	0.6371	1.404	7.511	0.0252	0.531	1.07	1916	2368	579096576
81	200	16	0.2294	1.636	0.0880	27.00	0.6091	1.406	8.511	0.0250	0.531	1.05	1835	2374	574182400
94	300	16	0.2228	1.662	0.0855	26.30	0.6110	1.412	9.511	0.0243	0.529	1.00	1847	2390	552950865

Table 4 (continued)

Run No.	Electrode Width mm	Free Height cm	$CuSO_4$ molarity	H_2SO_4 molarity	ΔC H_2SO_4 moles/liter	Limiting Current Density - ma/cm^2	Mass Transfer Coefficient x 10^3 - cm/sec	Average Viscosity centipoise	Bulk Density gm/cm^3	$\Delta \rho$ gm/cm^3	Average Diffusion Coefficient x 10^5 cm^2/sec	Transference No. $CuSO_4$ x 10^3	Nu'	Sc	Gr
114	5	1	0.6921	1.480	0.2289	123.00	0.9176	1.561	3.112	0.0835	0.481	3.48	190	2840	397787
123	5*	1	0.6644	1.500	0.2217	121.00	0.9405	1.553	3.122	0.0797	0.483	3.29	194	2816	382621
126	20	1	0.6644	1.500	0.2217	120.00	0.9327	1.553	5.112	0.0797	0.483	3.29	192	2816	382620
128	20*	1	0.6644	1.500	0.2217	120.00	0.9327	1.553	5.122	0.0797	0.483	3.29	192	2816	382620
134	100*	1	0.6570	1.530	0.2193	104.40	0.8207	1.559	7.122	0.0787	0.481	3.16	170	2833	375380
118	5	8	0.6849	1.490	0.2270	129.00	0.9725	1.560	3.412	0.0825	0.481	3.42	1615	2838	201358131
122	5*	8	0.6699	1.490	0.2232	123.00	0.9481	1.553	3.422	0.0805	0.483	3.35	1568	2815	197764300
130	20	8	0.6620	1.510	0.2209	122.00	0.9517	1.555	5.412	0.0794	0.482	3.24	1576	2822	194661760
132	20*	8	0.6593	1.520	0.2201	124.00	0.9713	1.557	5.422	0.0791	0.482	3.20	1610	2827	193413760
138	100*	8	0.6565	1.530	0.2192	103.40	0.8135	1.559	7.422	0.0787	0.481	3.15	1350	2832	192096768
251	1	1	0.3709¤	0.770	0.1683	26.20	0.3648	8.211	1.113	0.0395	0.133	3.27	272	52571	6816
248	2	1	0.3709¤	0.770	0.1683	18.30	0.2548	8.211	2.113	0.0395	0.133	3.27	190	52571	6816
247	5	1	0.3709¤	0.770	0.1683	16.70	0.2325	8.211	3.113	0.0395	0.133	3.27	173	52571	6816
252	5*	1	0.3709¤	0.770	0.1683	16.00	0.2227	8.211	3.123	0.0395	0.133	3.27	166	52571	6816
239	20	1	0.3700¤	0.759	0.1677	14.30	0.1995	7.964	5.113	0.0394	0.137	3.28	145	49944	7202
241	20*	1	0.3700¤	0.759	0.1677	14.50	0.2023	7.964	5.123	0.0394	0.137	3.28	147	49944	7202
233	100	1	0.3732¤	0.753	0.1694	14.50	0.2006	8.155	7.113	0.0397	0.134	3.32	149	52002	6945
236	100*	1	0.3732¤	0.753	0.1694	14.30	0.1978	8.155	7.123	0.0397	0.134	3.32	147	52002	6945
263	5	8	0.3690¤	0.774	0.1674	17.20	0.2407	8.134	3.413	0.0393	0.134	3.24	1428	51734	3535324
265	5*	8	0.3687¤	0.778	0.1672	16.90	0.2367	8.111	3.423	0.0392	0.135	3.23	1401	51472	3551482
257	20	8	0.3700¤	0.774	0.1679	13.90	0.1940	8.183	5.413	0.0394	0.134	3.25	1156	52256	3504757
259	20*	8	0.3696¤	0.775	0.1677	13.80	0.1928	8.159	5.423	0.0393	0.134	3.25	1146	51991	3521904
253	100	8	0.3706¤	0.771	0.1682	12.56	0.1750	8.207	7.413	0.0394	0.133	3.26	1045	52517	3491179
255	100*	8	0.3703¤	0.773	0.1680	12.80	0.1785	8.182	7.423	0.0394	0.134	3.26	1063	52257	3508326

All runs 22°C * with end walls ¤ 5.41 M Glycerol

Table 4 (concluded)

ZN-1644

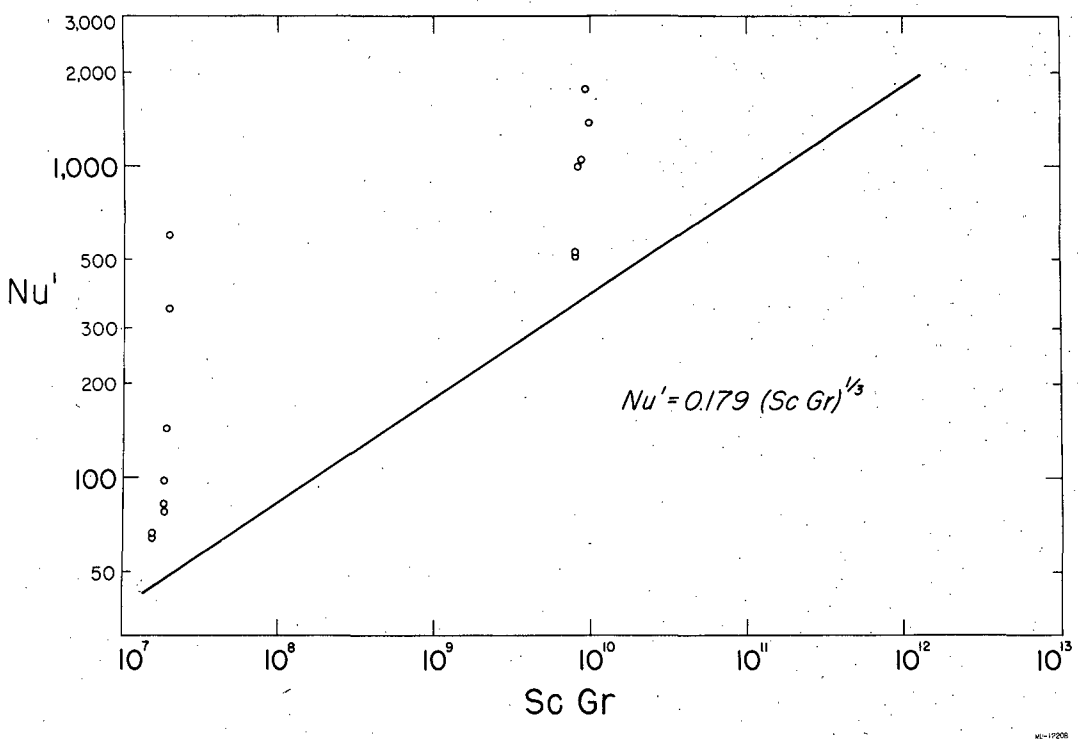

Fig. 19. Experimental points of 0.01 M $CuSO_4$ concentration presented with the general correlation of Figure 18.

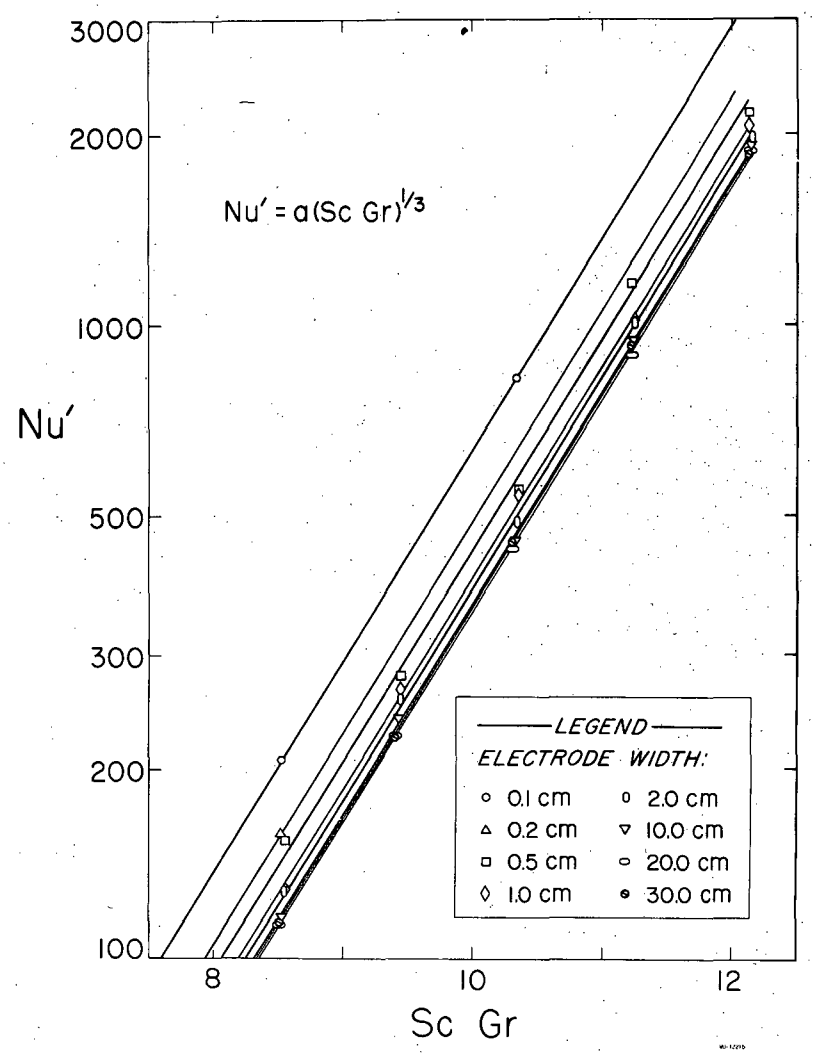

Fig. 20. Individual least square correlations for each electrode size (0.24 M $CuSO_4$ concentration).

electrode as well as smoothed values obtained from figure 21. With figure 21 as a basis, a corrected Nusselt number for mass transfer, Nu", was calculated by the equation

$$Nu'' = (a_{\infty} / a_x) \; Nu' \qquad (13)$$

Table 5

Electrode	"a" calculated	"a" smoothed	a_{∞} / a_x smoothed
0.1 cm.	0.2930	0.2930	0.5631
0.2 cm.	0.2265	0.2265	0.7284
0.5 cm.	0.2008	0.2008	0.8217
1.0 cm.	0.1846	0.1870	0.8823
2.0 cm.	0.1774	0.1756	0.9396
5.0 cm.	0.1581	0.1699	0.9712
10.0 cm.	0.1680	0.1668	0.9892
20.0 cm.	0.1642	0.1661	0.9934
30.0 cm.	0.1665	0.1654	0.9975
∞	-	0.1650	1.0000

The last column in Table 5 gives the smoothed values for the correction coefficient in equation 13. Figure 22 shows the correlation, using the corrected Nusselt number. In this case the least square method yields the equation

$$Nu'' = 0.165 \; (Sc \; Gr)^{1/3} \qquad (14)$$

As apparent from figure 22, the points for the runs with glycerol added are above the least square line. If one follows the suggestion of Schmidt,[14] and raises the Schmidt group to a power different than that of the Grashof number, a better correlation is obtained. Figure 23 was plotted from the equation

$$Nu'' = 0.129 \; (Sc^{1.1} \; Gr)^{1/3} \qquad (15)^*$$

Discussion of Correlation

The degree with which each of the three successive correlations, presented herein, represents the data, has been estimated by the

* The actual least square exponent on the Schmidt number should be 1.14.

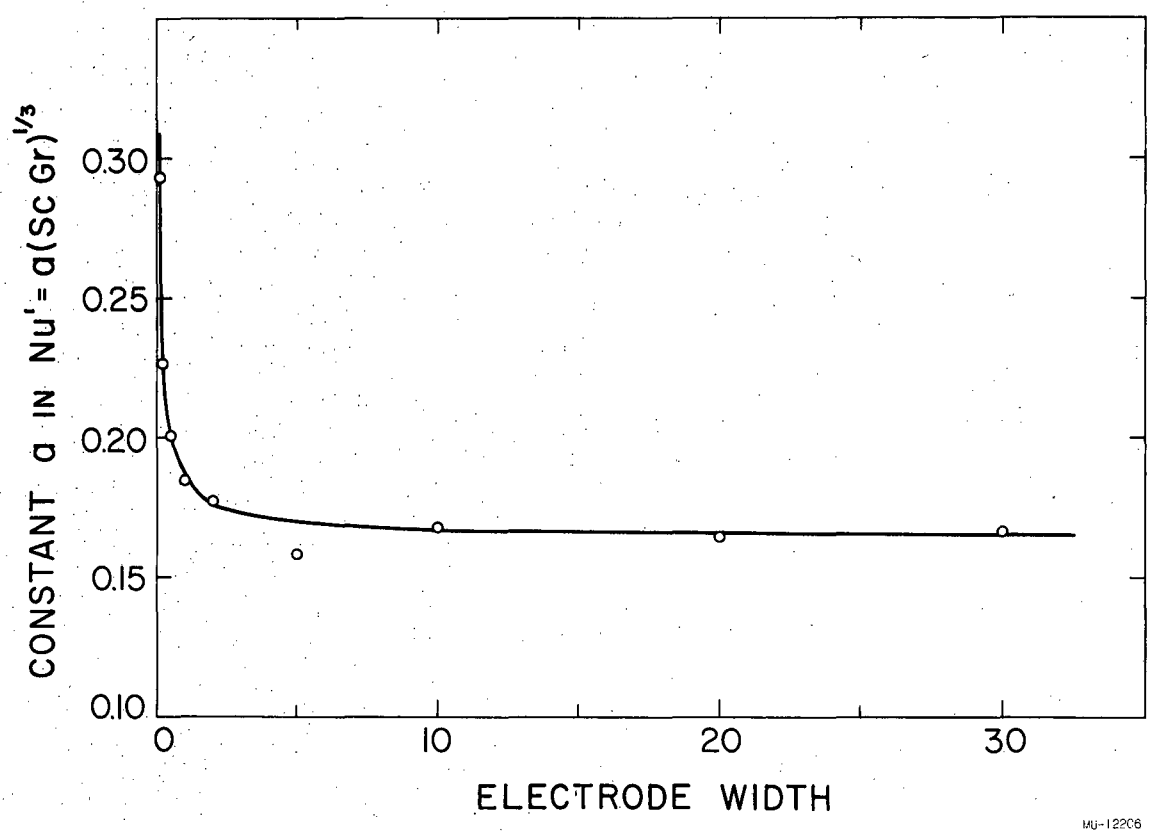

Fig. 21. Variation of intercept "a" as a function of electrode size (see Figure 20).

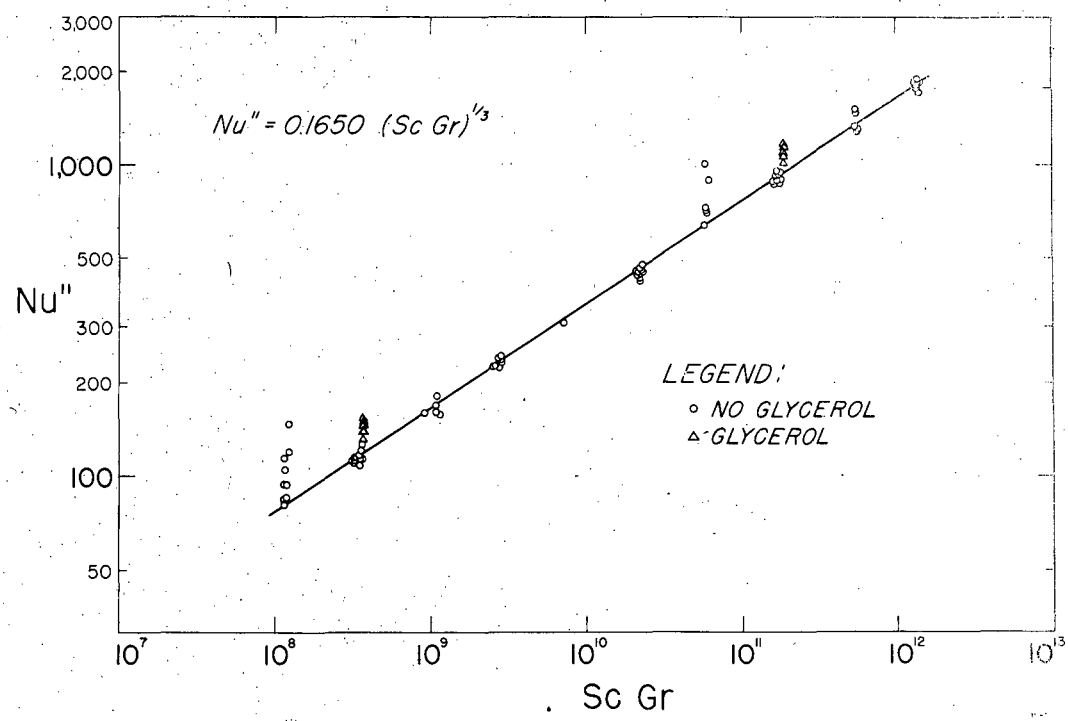

Fig. 22. General correlation, corrected for electrode size.

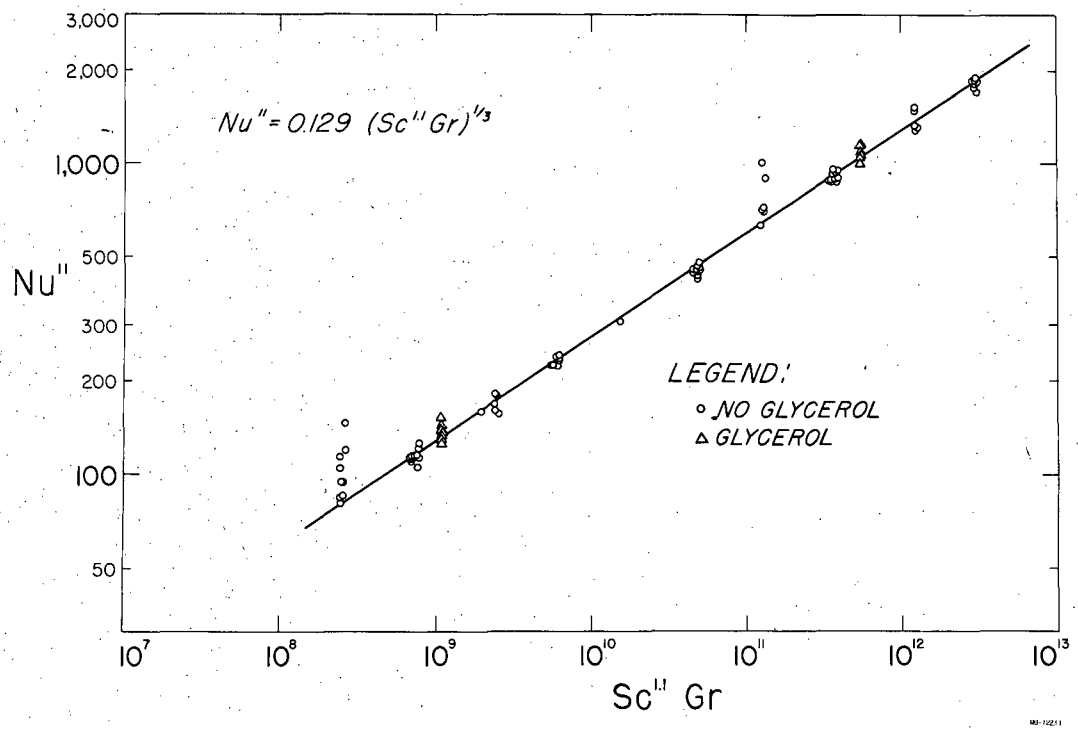

Fig. 23. General correlation, corrected for electrode size, and viscosity.

calculation of correlation coefficients, r*. These correlation coefficients are given in Table 6. The square of the correlation coefficient, r^2, also given in the table, is a more direct measure of the fit.

Table 6

Equation	Correlation Coefficient	(Correlation Coefficient)^2
12	0.978	0.956
14	0.990	0.981
15	0.992	0.985

For example for equation 15, the correlation coefficient is 0.985, which means that 98.5% of the experimentally determined dependance of Nu' on the Sc-Gr group is explained by the least square line. The remaining percentage must be explained in some other manner, such as by experimental error, or by the influence of other variables, not considered in this treatment.

Comparison of equations 12 – 15 points to a definite analogy between the heat and mass transfer case at horizontal surface in free convection. For the case of boiling water from a horizontal heated plate, Jakob and Linke[21] have correlated their data in the form

$$Nu = 0.273\ (\ Pr\ Gr\ )^{1/3} \tag{16}$$

According to Jakob,[22] "... except for very vehement boiling, the mechanism of convection in boiling is almost the same as for free convection of not boiling liquids." For the turbulent range, for heat transfer from vertical walls, Jakob also gives the equation

$$Nu = 0.129\ (\ Pr\ Gr\ )^{1/3} \tag{17}$$

It should be noted that the constant for horizontal plates is about twice that for vertical plates, which indicates that the efficiency of heat transfer is much larger in the former case. It is probable, however, that a considerable part of the difference is due to the effect

---

* For a discussion of correlation coefficients, any standard text on statistics may be consulted. As a specific reference, Bennett and Franklin,[20] page 37, is offered.

of bubbles formed on the horizontal surface. Jakob also indicates that a power on the Prandtl number will improve the correlation.

Conclusion

Equation 15 is presented as the correlation of limiting currents at horizontal electrodes under free convection conditions. Further, more elaborate investigation of the effect of electrode size (width) is desirable. It is assumed that the increase of mass transfer coefficient with decrease in width is principally due to the effect of "side currents" sweeping in from both sides from the bulk solution. This effect is noticeable only where the width of electrode is smaller than about 2 cm. Visual observation by means of Schlieren photographs or by photographing the path of suspended fine solid particles could give much needed information about the mechanisms involved near free edges and walls.

The effect of viscosity, also needs to be further clarified. Larger ranges of viscosities could be covered in a future experimental series in order to establish more accurately the proper exponent of the Schmidt group.

ACKNOWLEDGMENTS

The author wishes to express his gratitude to Dr. Charles Tobias, for his valued help and encouragement, and to Drs. P. B. Stuart and E. F. Orlemann for their critical review of this text.

Thanks is also extended to Mr. A. A. Franke for the many analysis, Mr. K. F. Hildebrand for the photography, and Miss Ruth Miller for the preparation of illustrations.

This work was performed under the auspices of the Atomic Energy Commission.

APPENDIX 1

Calculation of Dimensionless Numbers

The dimensionless numbers used in the correlations in this paper were calculated using the equation:

$$Nu' = k_L \times X_f / D_{Cu^{++}\,Av.} \tag{18}$$

$$Sc = \nu_{Av.} / D_{Cu^{++}\,Av.} \tag{19}$$

and

$$Gr = g(\rho_o - \rho_i)\, \rho^2_{Av.}\, x^3 / \rho_i\, \mu^2_{Av.} \tag{20}$$

where the mass transfer coefficient is calculated by

$$k_L = I_L\, (1 - t_{Cu^{++}\,Av.}) / n\, F\, C_{o\,Cu^{++}} \tag{21}$$

The film factor for the cupric ion in equation 18, for even the most concentrated cases, was so close to 1, due to the small volume of the copper ion, that unity was assumed. "x" is the characteristic length, which here is the free height above the electrode. In these equations the solution properties marked with the symbol "Av.", are properties obtained by averaging the value in the bulk solution and the value at the electrode surface.

In order to calculate the "Av.", it is necessary to know the composition at the surface of the electrode. At limiting current the concentration of cupric ions at the electrode surface is zero. However, due to the cathode reaction and migration, there is an increase in H_2SO_4 concentration at the surface of the electrode, which must be calculated. In steady state, the rate of movement of H_2SO_4 to the electrode by migration is equal to the rate at which it is transferred back to the bulk of the solution by diffusion and convection. Mathematically stated:

$$I_L\, t_{H^+Av.} = k_{H_2SO_4}\, (C_i - C_o)_{H_2SO_4} \tag{22}$$

There are three unknowns in this equation: the average transferrence number of the hydrogen ion, the mass transfer coefficient, and the interfacial concentration of H_2SO_4. If it is assumed that the mass transfer

coefficient for sulfuric acid bears the same relationship to its diffusivity as does that of copper sulfate, then from equation 15

$$k_{H_2SO_4} = (D_{H_2SO_4} / D_{CuSO_4})^{2/3}_{Av.} \; k_{CuSO_4} \qquad (23)$$

is obtained. With this equation, equation 21, and the equations relating diffusivity and transferrence number to concentration,* all unknowns can be solved for. The proceedure is a trial and error one, first assuming an interfacial concentration and, then, calculating it until the estimate and calculation agree.

Once the interfacial concentration is known, calculation of dimensionless groups is a matter of routine. The entire calculation was done by an IBM 650 electronic computer.

---

* See Appendix 2.

APPENDIX 2

Equations for Prediction of Physical Properties

In order to make the best use of the IBM 650 electronic calculator, it was necessary to set up equations relating the physical properties of the solutions to the concentration. The following set of equations* was derived for this purpose.

$$\rho = 0.9978 + 0.06406\, M_{H_2SO_4} - 0.00167\, M^2_{H_2SO_4} + 0.12755\, M_{CuSO_4} + 0.01820\, M^2_{CuSO_4} - 0.00235\, M_{Glycerol} + 0.00353\, M^2_{Glycerol} \quad (24)$$

$$\mu = 0.974 + 0.1235\, M_{H_2SO_4} + 0.0556\, M^2_{H_2SO_4} + 0.5344\, M_{CuSO_4} + 0.5356\, M^2_{CuSO_4} + 0.1475\, M_{Glycerol} + 0.2029\, M^2_{Glycerol} \quad (25)$$

$$\mu\, D_{CuSO_4} = (0.7363 + 0.00511\, M_{H_2SO_4} + 0.02044\, M_{CuSO_4} + 0.06530\, M_{Glycerol})10^{-5} \quad (26)$$

$$\mu\, D_{H_2SO_4} = (1.6691 + 0.24519\, M_{H_2SO_4} + 0.96637\, M_{CuSO_4} + 0.06530\, M_{Glycerol})10^{-5} \quad (27)$$

$$t_{Cu^{++}} = (0.2633 - 0.1020\, M_{H_2SO_4})\, M_{Cu^{++}} \quad (28)$$

$$t_{H^+} = 0.8156 - 0.2599\, M_{Cu^{++}} - 0.1089\, M^2_{Cu^{++}} \quad (29)$$

---

* Equations are for 22°C.

These equations were obtained by assuming power series behavior. Maximum deviation of calculated points from curves was within ± 1/2% in the concentration range used.

The data for the density and viscosity equations were taken by Eisenberg, Tobias, and Wilke.[23] Data published by Gordon and Cole,[24] Gordon,[25] and Thovert[26] corrected for ionic strength,[4] were used in estimating diffusivities.

Transference numbers were estimated on the assumption that, (1) sulfuric acid dissociated completely to hydrogen and bisulfate ions,[27] (2) bisulfate ion dissociated to hydrogen and sulfate ions with an equilibrium constant 2×10^{-2}, (3) copper sulfate dissociated completely to cupric and sulfate ions, and (4) ionic mobilities in concentrated solutions were equal to the ratio of ionic conductance in concentrated solution to ionic conductance at infinite dilution multiplied by the ionic mobility at infinite dilution. Ionization constants were obtained from the Handbook of Chemistry and Physics.[27] Ionic mobilities at infinite dilution were from Glasstone,[28] ionic conductances from Landolt Boernstein.[29] Transference numbers were calculated by:

$$t_i = C_i z_i u_i / C_1 z_1 u_1 + C_2 z_2 u_2 + \text{etc.} \qquad (30)$$

APPENDIX 3

Purity of Chemicals

Cupric Sulfate Anhyd. "Baker's Analyzed"

Analysis of Lot No. 41647

Chloride (Cl)	0.001%
Subst. not ppt. by H_2S	0.008%
Iron (Fe)	0.005%
Ammonium Sulfide Metals other than Fe (as Ni)	0.006%

Sulfuric Acid C. P. Garde

Maximum limits of impurities

Residue after Ignition	0.0004%
Chloride (Cl)	0.00002%
Nitrate (NO_3)	0.00002%
Ammonium (NH_4)	0.0001%
Substances reducing KMnO (as SO_2)	0.0001%
Arsenic (As)	0.0000005%
Heavy Metals (as Pb)	0.00008%
Iron (Fe)	0.00002%

NOMENCLATURE

Symbol	Definition	Units
a or x or ∞	Constant in correlation equation	--
a_i or o	Activity	--
b	Constant	--
c	Constant exponent	--
c_p	Heat capacity	cal/gm °C
C	Concentration	moles/liter
D	Diffusion coefficient	cm^2/sec
E	Polarization	volts
g	Acceleration of gravity	981 cm/sec^2
h	Heat transfer coefficient	cal/cm^2 °C sec
I	Current	amps
I_L	Limiting current density	amps/cm^2
k	Heat conductivity	cal/cm^2 sec °C/cm
k_L	Overall mass transfer coefficient	equiv/sec cm^2
$k_{Cu^{++}}$ or H^+	Mass transfer coefficient	equiv/sec cm^2
M	Molar concentration	moles/liter
n	Number of electrons exchanged in electrode reaction	--
R	Universal gas constant	1.987 cal/gm mole °C
T	Time	min
T	Temperature	°K
$t_{Cu^{++}}$ or H^+	Transference number	--
x	Characteristic dimension	cm
X_f	"film factor" for diffusion of Cupric ion	--

Greek letters

α	Thermal coefficient of expansion	1/°C
β	Temperature gradient	°C/cm
Δ	Signifies difference	--
$\kappa = k/\rho c_p$	Thermal diffusivity	cm^2/sec

(Nomenclature cont'd)

Symbol	Definition	Units
μ	Viscosity	gm/cm sec
$\nu = \mu/\rho$	Kinematic viscosity	cm^2/sec
ρ	Density	gm/cm^3

Subscripts

i	Interface	--
o	Bulk	--
Av.	Arithmetic average between bulk and interface	--
x	Electrode x cm. wide	--
∞	Infinite electrode	--

Dimensionless Groups

$Nu = hx/k$	Nusselt number for heat transfer
$Nu' = k_L x/D$	Nusselt number for mass transfer
$Nu'' = (a_\infty/a_x)\ Nu'$	Corrected Nusselt number for mass transfer
$Pr = \nu c_p/k$	Prandtl number
$Sc = \nu/D$	Schmidt number
$Gr = \dfrac{g(\rho_o - \rho_i)\rho^2 x^3}{\mu^2}$	Grashof number
$Ra = -\beta g \alpha x^4/K\nu$	Rayleigh number

LIST OF ILLUSTRATIONS

Figure	Caption	Page
1	Schematic diagram of Bénard cells: top, - plan view; bottom, - elevation. The arrows give the direction of flow	6
2	Heating current squared as a function of temperature difference between plates in heat transfer for two different plate separations	8
3	A limiting current curve, - electric current as a function of polarization voltage	12
4	Schematic diagram of experimental circuit	14
5	Experimental cell: top, - assembly photograph; bottom, section drawing	15
6	Example of each size electrode used	16
7	Cathode holder, in which each size electrode could be flush mounted	17
8	Top view of cathode in place, showing cathode contact and points at which reference cells could be attached	18
9	Reference electrodes	20
10	Assembled cell	21
11	General view of experimental area	22
12	Limiting current curves for different length runs with no other experimental variables changed	25
13	Variation of polarization with time at four points along a 20 cm. electrode	26
14	Limiting current density as a function of free space above the electrode for each concentration	28
15	Limiting current density as a function of width of electrode for each concentration	30
16	Typical limiting current curve for 0.01 M $CuSO_4$ concentration	32
17	Typical variation of polarization with time for 0.01 M $CuSO_4$ concentration	33

18 General correlation, with free space above the electrode as characteristic dimension..... 36
19 Experimental points of 0.01 M $CuSO_4$ concentration presented with the general correlation of figure 18..... 41
20 Individual least square correlations for each electrode size (0.24 M $CuSO_4$ concentration)..... 42
21 Variation of intercept "a" as a function of electrode size (see figure 20)..... 44
22 General correlation, corrected for electrode size..... 45
23 General correlation, corrected for electrode size and viscosity..... 46

BIBLIOGRAPHY

1. M. Eisenberg, C. W. Tobias, and C. R. Wilke, J. Electrochemical Soc. 101, 306-319 (1954).
2. C. S. Lin, R. W. Moulton, and G. L. Putnam, Ind. Eng. Chem. 45, 636 (1953).
3. N. Ibl, Chimia, 9, 135 (1955).
4. C. R. Wilke, M. Eisenberg, and C. R. Tobias, J. Electrochemical Soc. 100, 513 (1953).
5. S. Ostrach, Nat. Advisory Comm. Aeronaut. Tech. Note 2645, Lewis Flight Propulsion Laboratory, Cleveland, Ohio, (February 1952).
6. H. Bénard, Rev. Gen. Sci. 12, 1261, 1309 (1900).
7. O. G. Sutton, Micrometeorology, McGraw-Hill Co., New York, 1953, p. 119.
8. Lord Rayleigh, Phil. Mag. 32, 529 (1916).
9. H. Jeffreys, Pro. Roy. Soc., Series A, 118, 195 (1928).
10. A. Pellew and R. V. Southwell, Pro. Roy. Soc., Series A, 176, 312 (1940).
11. R. J. Schmidt and S. W. Milverton, Pro. Roy. Soc., Series A, 152, 586 (1935).
12. R. J. Schmidt and O. A. Saunders, Pro. Roy. Soc., Series A, 165, 216 (1938).
13. W. V. R. Malkus, Pro. Roy. Soc., Series A, 225, 185 (1954).
14. E. Schmidt, Chimie Ingeniueur-Technik, 28, 175 (1956).
15. S. Levy, J. Applied Mech., to be published.
16. J. N. Agar and F. P. Bowden, Pro. Roy. Soc., 169A, 206 (1938).
17. M. Eisenberg, "Studies on the Role of Ionic Diffusion and Mass Transfer in Electrode Processes," M. S. Thesis, University of California, Berkeley, California (1951).
18. I. M. Kolthoff and E. B. Sandell, "Textbook of Quantitative Inorganic Analysis," Macmillan, New York, 1949, p 630.
19. G. F. Smith, "Cerate Oxidimetry," G. F. Smith, Columbus, Ohio, 1942, p 92.
20. C. A. Bennett and N. L. Franklin, "Statistical Analysis in Chemistry and the Chemical Industry," Wiley, New York, 1954, p 37.

21. M. Jakob and W. Linke, Forschung a. d. Geb. D. Ingenieurwes, 4, 75, (1933).

22. M. Jakob, Heat Transfer, Wiley, New York, 1949, Vol. 1, p 526-534.

23. M. Eisenberg, C. W. Tobias, and C. R. Wilke, J. Electrochemical Soc., 103, 413 (1956).

24. A. R. Gordon and A. Cole, J. Phys. Chem. 40, 733 (1936).

25. A. R. Gordon, J. Chem. Phys. 7, 89 (1939); 8, 423 (1940).

26. G. Thovert, Landolt-Boernstein Tabellen, Vol. I, p 248.

27. Handbook of Chemistry and Physics, 33rd Edition, 1951-1952, p 1506-1510.

28. S. Glasstone, Introduction to Electrochemistry, Van Nostrand, New York, 1942, p 60.

29. Landolt-Boernstein Tabellen, Vol. 2, p 1070 - 1080.